Spatio-Temporal 4D Phenotyping for Automated Morphological Genotype Differentiation of Sugar Beet

Jonas Bömer

boemer@ifz-goettingen.de

Institute of Sugar Beet Research https://orcid.org/0000-0003-0723-4224

Elias Marks

Center for Robotics, University of Bonn https://orcid.org/0000-0003-1322-9317

Facundo Ramón Ispizua Yamati

Institute of Sugar Beet Research https://orcid.org/0000-0001-5775-3554

Cyrill Stachniss

Center for Robotics, University of Bonn https://orcid.org/0000-0003-1173-6972

Stefan Paulus

Institute of Sugar Beet Research https://orcid.org/0000-0003-4402-4760

Anne-Katrin Mahlein

Institute of Sugar Beet Research https://orcid.org/0000-0003-1091-3690

Research Article

Keywords: plant phenotyping, time series clustering, point cloud, laser scanning, variety approval

Posted Date: September 22nd, 2025

DOI: https://doi.org/10.21203/rs.3.rs-6700539/v2

Additional Declarations: The authors declare no competing interests.

Spatio-Temporal 4D Phenotyping for Automated Morphological Genotype Differentiation of Sugar Beet

Jonas Bömer[1]*, Elias Marks[2], Facundo Ramón Ispizua Yamati[1], Cyrill Stachniss[2], Stefan Paulus[1], Anne-Katrin Mahlein[1]

[1]Institute of Sugar Beet Research, 37079 Göttingen, Germany
[2]Center for Robotics, University of Bonn, 53115 Bonn, Germany
*Corresponding author. E-mail: boemer@ifz-goettingen.de

ORCIDs:
Jonas Bömer: 0000-0003-0723-4224, Elias Marks: 0000-0003-1322-9317, Facundo Ramón Ispizua Yamati: 0000-0001-5775-3554, Cyrill Stachniss: 0000-0003-1173-6972, Stefan Paulus: 0000-0003-4402-4760, Anne-Katrin Mahlein: 0000-0003-1091-3690

Abstract

Purpose 3D models are used in plant phenotyping for non-destructive quantification and analysis of morphological characteristics. Analyzing plant structure allows breeders to select for desirable traits, associated with e.g. drought tolerance or increased productivity. In sugar beet, morphological parameters depict an essential element of the variety approval for distinguishing between genotypes. However, only a limited number of measured or scored parameters are considered at a single time point. This study aims to disclose the benefit of incorporating dynamic spatio-temporal development of 3D parameters for automated crop genotype differentiation.

Methods A greenhouse experiment was conducted covering twelve sugar beet genotypes. High-resolution 3D models were generated twice a week over the course of two months and both common and novel 3D morphological parameters were extracted. The importance of these parameters was assessed over time, and the dataset was analyzed using unsupervised pointwise clustering and time series clustering.

Results Varying importance of parameters depending on the time point and the noticeable higher importance of plant parameters compared to leaf parameters are demonstrated by our results. Moreover, increased and more stable genotype differentiation is archived using time series clustering compared to pointwise clustering. Furthermore, taproot formation of sugar beet was found to have a crucial impact on morphological development.

Conclusions Substantial genotypic variations in the dynamic development of 3D morphological parameters could be demonstrated. The higher and more stable clustering performance using time series analysis underlines the importance of 4D data for plant genotype differentiation. Future work should focus on identifying important growth stages for data collection.

Keywords

plant phenotyping, time series clustering, point cloud, laser scanning, variety approval

Statements and Declarations

The authors declare that they have no conflict of interest.

Acknowledgements

We would like to express our gratitude to the German Federal Plant Variety Office for their expertise and support in conducting the greenhouse trials. Furthermore, we would like to acknowledge the contributions of all colleagues at IfZ, who contributed in maintaining the experiments, collecting the data and proofreading the manuscript. We would especially like to recognize Saskia Flentje's exceptional efforts in manually labeling the collected point cloud dataset.

Author contributions

Conceptualization: Jonas Bömer, Facundo Ramón Ispizua Yamati, Elias Marks; Methodology: Jonas Bömer, Facundo Ramón Ispizua Yamati, Elias Marks; Formal analysis and investigation: Jonas Bömer, Elias Marks; Writing - original draft preparation: Jonas Bömer; Writing - review and editing: all authors; Funding acquisition: Anne-Katrin Mahlein, Stefan Paulus, Cyrill Stachniss; Supervision: Anne-Katrin Mahlein.

Funding

The project was supported by funds of the Federal Ministry of Food and Agriculture (BMEL) based on a decision of the Parliament of the Federal Republic of Germany. The Federal Office for Agriculture and Food (BLE) provides coordinating support for artificial intelligence (AI) in agriculture as funding organisation, grant number 28DK108C20 - RegisTer.

This work has been funded by the Deutsche Forschungsgemeinschaft (DFG, German Research Foundation) under Germany's Excellence Strategy – EXC 2070 – 390732324 - PhenoRob.

The project was supported by funds of the Federal Ministry of Food and Agriculture (BMEL) based on a decision of the parliament of the Federal Republic of Germany via the Federal Office for Agriculture and Food (BLE) under the strategy for digitalisation in agriculture FKZ 28DE104A18 – FarmerSpace.

Introduction

Modern approaches in plant phenotyping mainly focus on high-throughput measurement systems and non-destructive measurement of plant traits over time. Costa et al. (2019) described these developments as a crucial step towards future advancements in modern plant breeding. Furthermore, plant breeding is a highly labor-intensive process, which makes automation essential (Fiorani et al., 2013). Phenotyping accesses complex morphological or biological plant traits to measure their current status and development, for instance, gaining knowledge about plant responses to stress factors or predicted yield on different scales (Fiorani et al., 2013; Li et al., 2014). Consequently, phenotyping offers invaluable insight to breeders, enabling them to make optimized selections in long-term breeding processes. Traditional phenotyping, which relies on manual measurements and visual scoring approaches, has undergone dramatic changes in recent years by utilizing state-of-the-art sensors and analysis techniques (Kim, 2020; Pieruschka et al., 2019; Walter et al., 2015).

The study of plant morphology is not only a valuable tool in the field of plant breeding, but also an essential component in the process of variety approval, a prerequisite for commercial marketing of crops in the European Union. The Community Plant Variety Office provides a set of standardized test protocols for all major crops, which are designed to assess the distinctness, uniformity, and stability of a proposed genotype. These protocols define a carefully selected set of parameters to assess important morphological parameters like plant height (e.g. for wheat (Community Plant Variety Office, 2019), maize (Community Plant Variety Office, 2010), rapeseed (Community Plant Variety Office, 2025a)) or more fine-grained parameters like leaf length, width or attitude (e.g. for tomato (Community Plant Variety Office, 2025c), sweet pepper (Community Plant Variety Office, 2025b), sugar beet (Community Plant Variety Office, 2018)). Sugar beet (*Beta vulgaris*) plays a distinctive role in this process, as it demands a diverse set of characteristics for approval. It should be noted, however, that within this process, morphological parameters of sugar beet are only accessed at a single point in time.

A primary objective of both plant breeding and variety approval is to differentiate between different genotypes, based on quantifiable morphological parameters. Today, the necessary parameters are obtained through manual techniques, including counting, scoring, and measuring. This involves both, a time-consuming and labor-intensive process that cannot be reviewed or checked retrospectively. As indicated by Awada et al. (2018), plant breeding has not yet fully integrated numerous emerging technologies associated with digital plant phenotyping. This also applies to the variety approval process for sugar beet (Manthey et al., 2021),

which represents a promising opportunity for the digitalization of data collection in order to gain more detailed and comprehensible information. For most morphological parameters, a digital survey can be effectively fulfilled by recording three-dimensional (3D) data and a subsequent computer-aided analysis.

The acquisition of 3D data and subsequent extraction of morphological parameters have gained increasing importance over the past decade, forming the field of 3D plant phenotyping (Akhtar et al., 2024; Paulus, 2019). 3D data provides a comprehensive description of a crop's geometry, and in comparison to two-dimensional (2D) imaging, it enables the description of more complex parameters, such as the volume of a plant or the angle of its leaves. The necessity for 3D measurements of crop structures at varying scales, from individual leaves to entire canopies, was already highlighted by Biskup et al. (2007) and Paproki et al. (2012) in the last decade. Since then, the demand for such measurements has grown, driven not only by technical advancements and the increased affordability of 3D sensor technology and computational resources (Fiorani et al., 2013), but also due to the deployment of advanced analysis techniques that utilize Machine Learning algorithms for the processing and interpretation of multidimensional data (Tardieu et al., 2017). Nowadays, the field of 3D plant phenotyping encompasses a wide spectrum of sub-disciplines, including but not limited to plant growth monitoring or environmental stress response analysis (Harandi et al., 2023).

A number of studies have addressed the topic of utilizing 3D data for differentiation tasks in the field of agriculture. Weiss et al. (2010) investigated the classification of diverse plant species based on coarsely resolved laser-scanned point clouds. They highlighted the significant challenge posed by the morphological similarity across species in the automatic differentiation of plant species. The researchers accessed reflectance-based, 3D, and 2D parameters at the single plant scale and reported, in addition to a species classification accuracy of 98 %, high importance of 3D point distribution parameters. In a study by Strothmann et al. (2017), multi-wavelength 3D data were employed for the classification of plant species, with a particular focus on differentiating between crops and weeds in field environments. The findings demonstrate the efficacy of 3D features for real-time species discrimination in challenging field conditions, highlighting the significant information content of plant morphology for differentiation tasks. Furthermore, Young et al. (2023) utilized morphological parameters extracted from the canopy of soybean plants to describe their diversity and build a database to identify genotypes with similar-shaped canopies.

Upon reconsidering the initial statement by Costa et al. (2019), it becomes evident that modern phenotyping emphasizes non-destructive trait measurement over time. However, the temporal development of 3D morphological parameters, particularly in the context of genotype differentiation, remains largely unexplored.

The non-invasive nature of 3D measurements can only be adequately utilized if the temporal dimension is fully considered. This implies that a parameter's dynamic development must be considered to fully leverage the potential of these digital measurement techniques.

Furthermore, the lack of studies focusing on spatio-temporal genotype differentiation is also evident in the limited availability of public datasets. As shown by Lu et al. (2020), there is a shortage of publicly accessible 3D datasets of plants that encompass a substantial number of genotypes and repetitions, coupled with temporal data acquisition. For instance, the Pheno4D dataset (Schunck et al., 2021) and a recently published dataset by James et al. (2025) provide temporal data of crops in addition to detailed semantic labels. However, they lack sufficient genotypes and repetitions to make a meaningful contribution to the research field in question. The 3D dataset of field-grown sugar beet provided by Marks et al. (2024) includes a substantial number of genotypes and additional plant and leaf labels. However, it covers only one point in time and thus lacks the ability to analyze four-dimensional (4D) temporal parameter development.

Nevertheless, the temporal development of crops holds valuable information, and its use is not limited to genotype differentiation. It can also be employed to improve disease detection in crops (Ispizua Yamati et al., 2024) or determine their ripeness (Kierdorf et al., 2023, 2024). In their study, Taghavi Namin et al. (2018) employed time series 2D image data in combination with Deep Learning techniques, both with and without Long Short-Term Memory, to distinguish between four distinct *Arabidopsis thaliana* genotypes. The authors concluded that the incorporation of temporal information resulted in enhanced classification accuracy, thereby underscoring the significance of temporal data for genotype differentiation. Moreover, Zhu et al. (2020) examined the development of 3D parameters of the leaf apparatus of soybean over the course of its full growth period. A continuous data collection approach was employed, enabling the generation of visual representations of the parameter development of different genotypes utilizing radar charts. The authors note that the genotypes exhibited notable differences in parameter development and discussed the potential use of this information in precision agriculture for precise water and fertilizer application. Furthermore, Ma et al. (2025) investigated the dynamic development of 3D morphological parameters of different lettuce genotypes over time. They were able to visualize significant differences in the parameter expression for plant height and plant width. While both studies accessed and illustrated the dynamic development of morphological parameters of crops, they did not utilize this data for further analysis regarding genotype differentiation, leaving the potential impact of spatio-temporal data unexplored.

The main contribution of our study is provided by the assessment of the dynamic development of 3D morphological parameters over time for the process of plant genotype differentiation. A spatio-temporal 4D examination of the differentiation task is enabled by the incorporation of the temporal dimension, thereby providing a more comprehensive view of the proposed topic. To investigate the temporal aspect of genotype differentiation, the development of twelve different sugar beet genotypes was analyzed over a two-month period. A total of 58 morphological 3D parameters were extracted on plant and leaf scale and their importance for genotype differentiation was investigated. Thus, a valuable contribution is made by our exploration of 3D parametrization of crops and the identification of important morphological parameters for genotype differentiation of sugar beet depending on the growth stage. Furthermore, the importance of the different observation scales is elucidated by our comparison of the influence of plant and leaf parameters. To finally quantify the impact of spatio-temporal plant phenotyping for genotype differentiation, the extracted parameters were analyzed using two unsupervised clustering algorithms with and without the capability of considering temporal parameter dynamics. The importance of incorporating temporal information is illustrated by our study, thereby establishing a foundation for the informed utilization of the spatio-temporal development of 3D morphological parameters in plant phenotyping. Advancements in plant breeding and the approval process for new crop genotypes will be facilitated by our findings.

Materials and methods

Experimental Design

The experimental data were collected in a controlled greenhouse environment conducted in Göttingen, Germany, in November and December 2021. The greenhouse was set to a constant temperature of 24°C and an artificial illumination cycle of 16 hours per day. Sugar beet plants were grown in two liter pots filled with a pre-fertilized soil mixture made from sand and topsoil. A standardized treatment protocol was implemented, including routine pest and disease control and fertilization to ensure consistent plant vitality. The spacing between the single pots was chosen large enough to ensure that the plants had enough space to grow without interruption by their neighbors. The experimental setup is depicted in Figure 1, including a visual representation of four analyzed sugar beet genotypes to demonstrate the morphological differences present in the dataset.

A total of twelve distinct sugar beet genotypes, categorized into two groups, were selected for analysis. A total of eight genotypes were selected which are utilized in sugar beet breeding and thus exhibit a high degree of

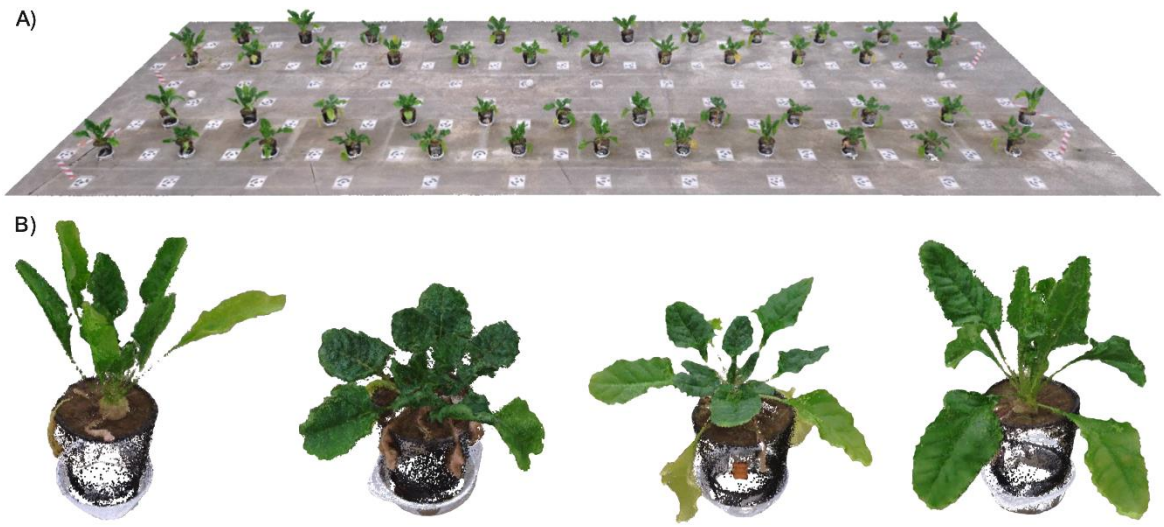

Figure 1: Three-dimensional model of the greenhouse experiment (A), created using a terrestrial laser scanner, including four close-ups of point clouds from different sugar beet genotypes cultivated in this study (B) (genotypes from left to right:1, 2, 9, 5), illustrating the wide range of morphological characteristics present in the collected dataset.

morphological diversity. Hereafter, these will be referred to as breeding genotypes. In contrast, four commercially available varieties were selected, hereafter referred to as market genotypes, which have passed federal variety approval and exhibit less distinct morphological differences. This combination allowed focusing on differences in parameter development while still maintaining the ability to transfer the results to more practical situations. The experiment was set up as a fully randomized block design with four repetitions, resulting in 48 cultivated plants. The 3D data were collected in the early morning hours to ensure an adequate turgor and to minimize any effects of the plant's water balance on the leaf attitude. To achieve this, the plants were watered each evening before data acquisition. The initial data collection occurred 37 days after sowing (DAS).

The 3D dataset comprises 16 time points, ranging from 37 to 93 DAS with intervals of three to four days. However, due to a malfunction of the utilized sensor, the interval between time points nine and ten is seven days.

3D Data Collection

The point cloud data were acquired using a Light Detection and Ranging (LiDAR) 3D scanner (Faro Focus S70; Faro Technologies Inc, Lake Mary, USA). The sensor exhibits a distance accuracy of ±1mm, an average point spacing of 3.1mm at a distance of 10m, and measures at a wavelength of 1550nm. The device was mounted in an upside-down orientation to an extension arm affixed to a tripod in a height of 1.8m (see Figure 2: Data Collection). This configuration provides a superior view of the innermost leaves and consequently reduces the occlusion factor.

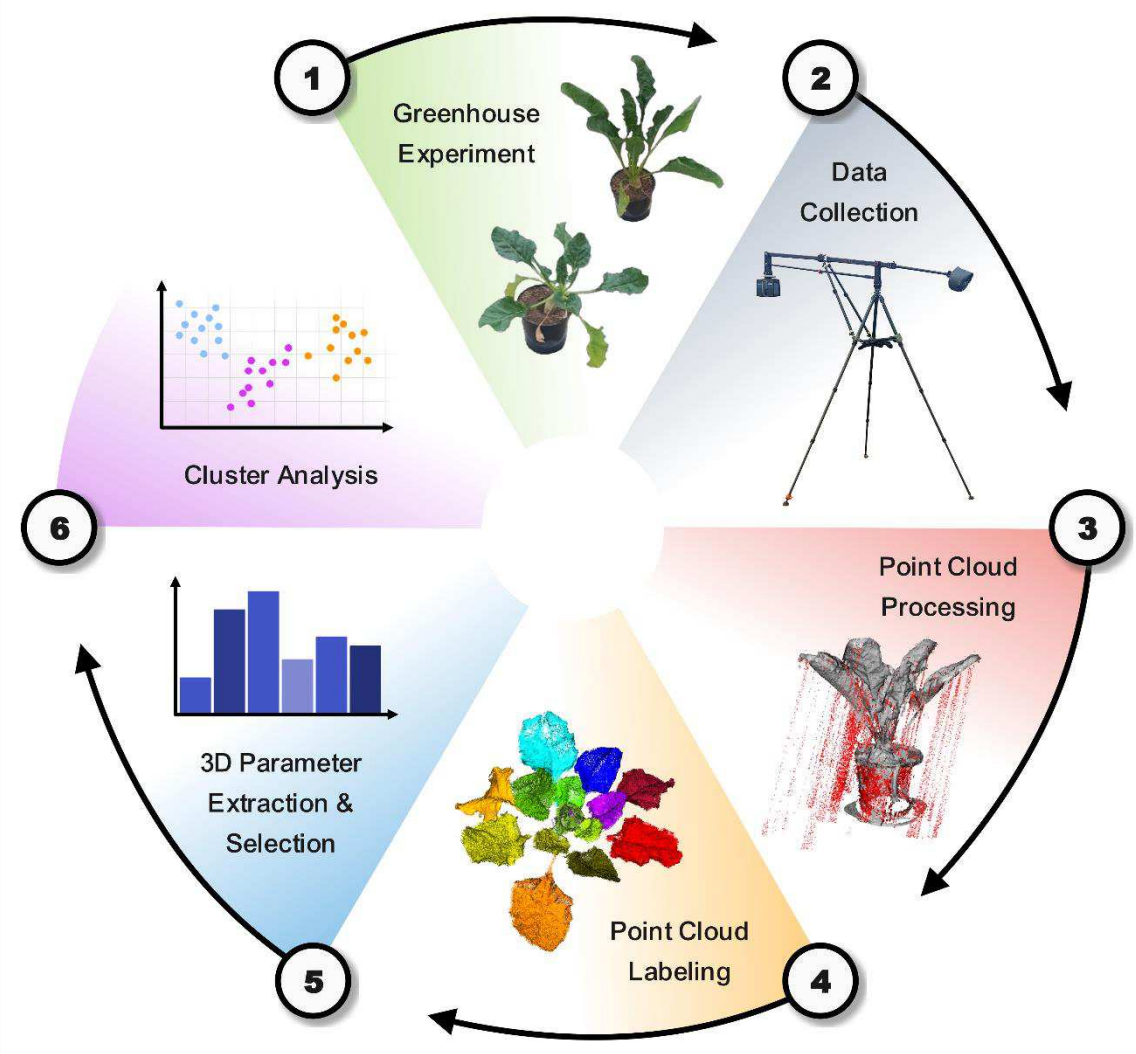

Figure 2: Key work packages of the study, illustrating the research workflow: 1) Greenhouse experiment with twelve genotypes, 2) Data collection using LiDAR setup, 3) Processing and preparation of the data into point clouds, 4) Labeling of individual plant organs, 5) Extraction and selection of 3D morphological parameters, and 6) Cluster analysis for unsupervised genotype differentiation.

To obtain 3D point clouds with minimal occlusion and high point density, ten individual scanning positions were arranged in a circle at equal intervals across the trial. The entire data acquisition process took approximately one hour. A total of nine spherical scanning targets (Ø 145mm; Laserscanning Europe GmbH, Magdeburg, Germany) were positioned in and around the trial for later registration of the single 3D scans into a complete 3D model.

3D Reconstruction

A 3D laser scanning software (Faro Scene; Faro Technologies Inc, Lake Mary, USA) was utilized to preprocess the single scans, applying stray point and edge filtering to eliminate larger noise in the point cloud. Subsequently, the spherical registration targets were marked, and the individual 3D scans were registered into a unified 3D point cloud with sub-millimeter point density. Next, the point clouds from each measurement

date were transformed into the same Cartesian coordinate system using three additional photogrammetric targets. This allowed for a straightforward extraction of individual plants on consecutive dates using predefined coordinates for each plant, as the pots remained stationary throughout the trial.

Software Dependencies

Further processing of the point clouds and the subsequent analysis were conducted in Python (v.3.10.0) (Van Rossum et al., 2009), beginning with the preprocessing of the extracted point clouds of individual plants from the greenhouse trail. Therefore, the libraries NumPy (v.1.26.4) (Harris et al., 2020) and Open3D (v.0.18.0) (Zhou et al., 2018) were used. Furthermore, Numpy, Open3D and SciPy (v.1.14.0) (Virtanen et al., 2020) were used to extract and validate morphological parameters. The final data analysis was conducted with the help of NumPy, pandas (v.2.2.2) (The pandas development team, 2024), scikit-learn (v.1.5.0) (Pedregosa et al., 2011), sktime (v.0.30.1) (Király et al., 2024), and umap (v.0.5.6) (McInnes et al., 2018). The results were visualized using Matplotlib (v.3.9.0) (Hunter, 2007).

Point Cloud Preprocessing

First, the point cloud of every single plant had to be extracted using manually annotated positions of the plant pots *xy*-coordinates. Subsequently, the floor was removed for every plant using the RANSAC algorithm (Fischler et al., 1987). After that, outliers were removed using a statistical outlier filter (Rusu et al., 2008) (see Figure 2: Point Cloud Processing).

Following the removal of outliers, the individual plant point clouds were manually labeled using an online labeling tool (Segments.ai, 2023). Each point cloud was labeled into pot, leaves, beet root, and core which was created for the most inner and undeveloped leaves that could not be labeled with sufficient certainty. The growth point of each plant was manually annotated in the first collected dataset as the point at which the plant emerges from the soil. Since the plant pots were not moved for the entirety of the experiment, the growth points could be extrapolated to subsequent time points.

3D Morphological Parameters

Definition and Extraction

The extracted morphological parameters include parameters such as plant height or width, which have been previously addressed in existing literature. Additionally, new parameters for 3D plant phenotyping were introduced, including those pertaining to the radial or spatial point distribution of a plant. To ensure the transferability of the knowledge gained to future research, including other crops, the generated parameters had

to meet specific criteria. They needed to be rotation-invariant, robust to extract, and applicable across plant genotypes and species.

The extracted parameters can be classified into two principal categories. The initial category is based on the individual plant, thus the parameters are designated as plant parameters (Figure 3). These can be obtained following the extraction of the individual plant's point cloud. To calculate plant parameters, it is necessary to utilize the point cloud data and, depending on the specific parameter being calculated, additional information about the growth point. Table 1 provides an overview of the extracted plant parameters and provides a detailed description of each parameter.

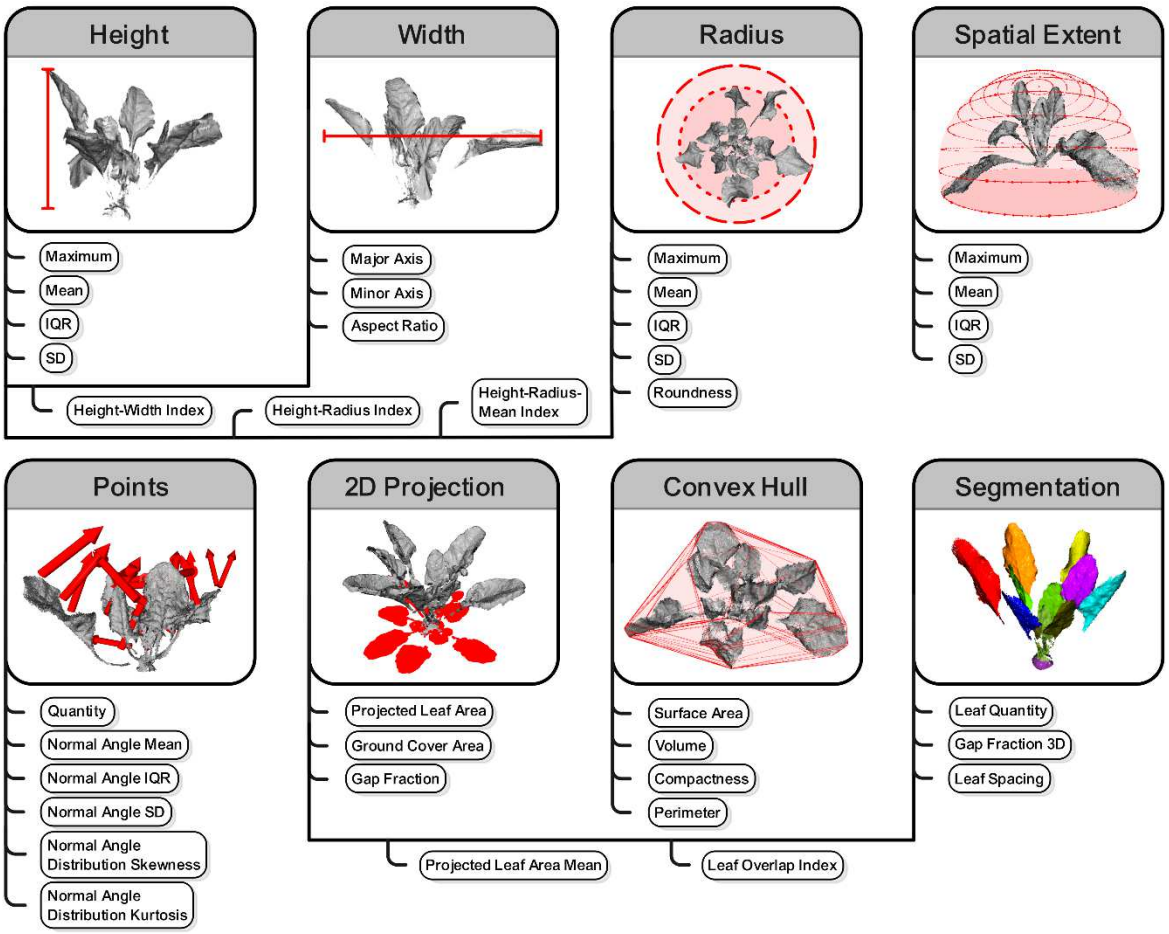

Figure 3: 3D morphological parameters of sugar beet at the level of a single plant. The illustration encompasses eight principal categories from which first-order 3D parameters can be directly derived (vertical). Additionally, there are second-order index parameters depicted that integrate individual parameters from multiple main categories (horizontal). (IQR: Interquartile Range, SD: Standard Deviation).

The second group of parameters examines the characteristics of individual leaves, which are subsequently designated as leaf parameters (Figure 4). To obtain these organ-specific parameters, pointwise annotations were required. As previously stated, leaf instance segmentation was conducted manually to circumvent issues pertaining to the quality of automatic labels. The data for generating the leaf parameters was extracted through the fitting of a digital leaf template to the point cloud of each leaf. The template contains predefined key points like the leaf blade base or the leaf tip for an easy assessment of morphological parameters. A more comprehensive understanding of this algorithm can be gained in Marks et al. (2022). The final leaf parameters for each plant were finally created by calculating multiple statistical values, including all leaves of a single plant. Table 2 provides an overview and a detailed definition of the extracted leaf parameters.

Table 1: Overview and detailed description of collected plant parameters. (IQR: Interquartile Range, SD: Standard Deviation).

Parameter	Definition
Height Maximum	99^{th} percentile of all Euclidean distances between $point_n$ and the growth point measured along the *z*-axis
Height Mean/IQR/SD	Descriptive statistics of all Euclidean distances between $point_n$ and the growth point measured along the *z*-axis
Width Major Axis	Maximum Euclidean distance between two points on the *xy*-plane
Width Minor Axis	Maximum Euclidean distance between two points on the *xy*-plane, orthogonal to the major axis
Width Aspect Ratio	Ratio of the minor axis length to the major axis length
Height-Width Index	Ratio of the maximum height to the major axis length
Radius Maximum	99^{th} percentile of all Euclidean distances between $point_n$ and the growth point measured on the *xy*-plane
Radius Mean/IQR/SD	Descriptive statistics of all Euclidean distances between $point_n$ and the growth point measured on the *xy*-plane
Roundness	Ratio of the maximum to the minimum Euclidean distance on the *xy*-plane between the growth point and the points of the perimeter of the point cloud
Height-Radius Index	Ratio of the maximum height to the maximum radius
Height-Radius-Mean Index	Ratio of the mean height to the mean radius
Spatial Extent Maximum	99^{th} percentile of all Euclidean distances between $point_n$ and the growth point measured in *xyz*-coordinate space
Spatial Extent Mean/IQR/SD	Descriptive statistics of all Euclidean distances between $point_n$ and the growth point measured in *xyz*-coordinate space
Points Quantity	Number of points after voxelization with a standardized voxel size
Normal Angle Mean/IQR/SD	Descriptive statistics of the angles between the *z*-axis and a points normal
Normal Angle Distribution Skewness	Asymmetry of the angle distribution between the *z*-axis and the point normals
Normal Angle Distribution Kurtosis	Flatness of the angle distribution between the *z*-axis and the point normals
Projected Leaf Area	Surface area of the point cloud projected on the *xy*-plane
Ground Cover Area	Surface area of the 2D convex hull of the point cloud projected on the *xy*-plane
Gap Fraction	Ratio of the projected leaf area to the ground cover area
Convex Hull Surface Area	Area of the smallest convex shape that can enclose the point cloud
Convex Hull Surface Volume	Volume of the smallest convex shape that can enclose the point cloud
Convex Hull Surface Compactness	Ratio of the convex hull volume to the convex hull surface area
Convex Hull Surface Perimeter	Perimeter of the 2D convex hull of the point cloud projected on the *xy*-plane
Leaf Quantity	Number of individual leaves of the point cloud
Gap Fraction 3D	Ratio of the summed-up 3D surface area to the ground cover area
Leaf Spacing	Mean Euclidean distance between each leaf and its closest three neigh- boring leaves in *xyz*-coordinate space
Projected Leaf Area Mean	Ratio of the projected leaf area to the number of leaves
Leaf Overlap Area	Ratio of the projected leaf area to the summed-up 3D surface area

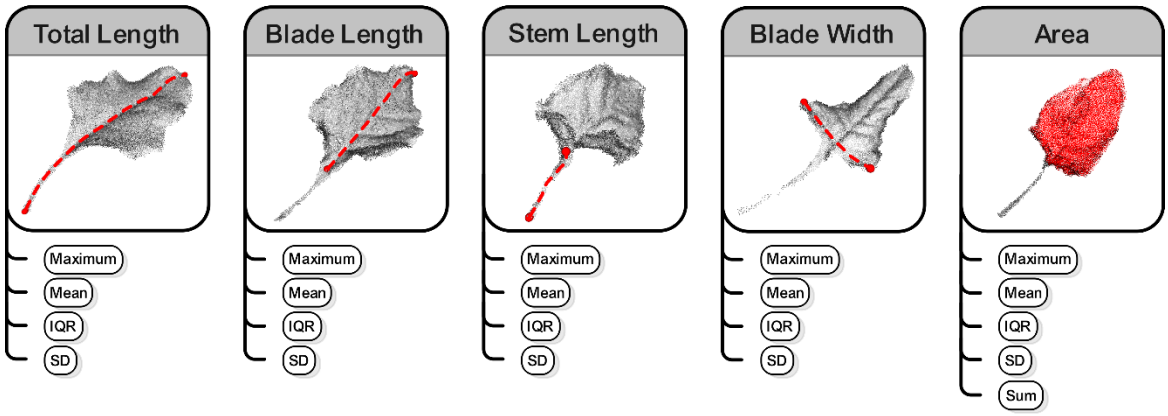

Figure 4: 3D morphological parameters of sugar beet at the level of a single leaf. In each instance, the measured distance or area is indicated in red. (IQR: Interquartile Range, SD: Standard Deviation).

A total of 58 morphological parameters were extracted from each plant's point cloud, composed of 37 plant and 21 leaf parameters. This effectively translated the enclosed information and reduced it to a lower dimensional representation.

Referencing and Validation

Henke et al. (2022) investigated the impact of geometric inaccuracies of 3D scans on morphological plant parameters. While some parameters, such as plant height, are robust to missing data, other parameters of higher dimensionality were more sensitive to the type and extent of geometric perturbation. To ensure the uniformity and accuracy of the parameter extraction pipeline, a 3D printed reference model of a sugar beet plant was employed in accordance with the methodology outlined by Bömer et al. (2024). The use of the reference model permits the comparison of extracted parameter values under varying data collection conditions, thereby facilitating an effective analysis of the consistency and precision of parameter extraction. Additionally, the model permits the inspection of morphological parameters that are not measurable with conventional, manual measurement methods (Bömer et al., 2024).

Table 2: Overview and detailed description of collected leaf parameters. (IQR: Interquartile Range, SD: Standard Deviation).

Parameter	Definition
Leaf Length Maximum/Mean/IQR/SD	Descriptive statistics of the measured geodesic distances between the growth point and the leaf tip for all leaves of a plant
Blade Length Maximum/Mean/IQR/SD	Descriptive statistics of the measured geodesic distances be-tween the leaf blade base and the leaf tip for all leaves of a plant
Stem Length Maximum/Mean/IQR/SD	Descriptive statistics of the measured geodesic distances between the growth point and the leaf blade base for all leaves of a plant
Blade Width Maximum/Mean/IQR/SD	Descriptive statistics of the maximum geodesic distances of the leaf blade measured orthogonal to the leaf major axis for all leaves of a plant
Leaf Area Maximum/Mean/IQR/SD/Sum	Descriptive statistics of the triangulated surface areas of the leaf blade for all leaves of a plant

The model was integrated into the data collection process by situating it in the greenhouse experiment at various locations at 15 time points, thereby providing a comprehensive illustration of diverse scanning scenarios, including variations in distance and angle between the sensor and the reference model. Subsequently, the point cloud of the reference model was extracted manually, and outliers were automatically removed using the described processing pipelines. Thereafter, the morphological parameters previously defined were extracted for each time point. To assess the consistency of parameter extraction, the Coefficient of Variation (CV) was employed using the following formula:

$$CV(\%) = \left(\frac{\sigma}{\mu}\right) \times 100 \quad (1)$$

where:

- σ is the standard deviation of all measurements
- μ is the mean of all measurements

The Mean Relative Error (MRE) was calculated to additionally assess the precision of the extracted values compared to the reference values of the model. The MRE was calculated as follows:

$$MRE(\%) = \frac{1}{n}\sum_{i=1}^{n}\left(\frac{m_i - t}{t} \times 100\right) \quad (2)$$

where:

- n is the number of measurements
- m_i is the i^{th} measurement
- t is the reference value

Parameters with a CV >10 % were excluded from further use, as their extraction was considered to be unstable. The determination of the appropriate CV for acceptance or rejection of a parameter is a challenging task, influenced by many factors (Pélabon et al., 2020). Nevertheless, a CV of less than 10 % is considered a relatively low level of variation (Lande, 1977), and errors up to 10 % can be considered acceptable for morphological phenotyping (Paproki et al., 2012).

A high MRE was not automatically used as an exclusion criterion when paired with a low CV, as this represents an observable difference between measured and benchmark values, but also a stable parameter

extraction. The MRE was used to identify technical inconsistency in the algorithms or database and extracted parameter values should not be compared between different datasets or studies. However, as long as the CV documents a stable parameter extraction, the parameter has been used for further analysis.

Statistical Analysis

Parameter Importance

To assess the impact of each extracted 3D morphological parameter on genotype differentiation and illustrate their impact over time, univariate feature importance was assessed for each parameter at each time point based on F-values derived from an analysis of variance. The restricted sample size of the experiment precluded the application of conventional model-specific feature importance metrics such as Random Forest Classifiers (Breiman, 2001) or model-agnostic approaches like SHAP (Lundberg et al., 2017). The univariate feature importance was assessed by evaluating the correlation between each feature and the target variable genotype, utilizing all twelve genotypes of the trial. The resulting F-statistics were used to generate an importance curve over time for each parameter.

Clustering

The extracted parameters were clustered using two distinct clustering approaches. The first approach utilized a common clustering algorithm for Pointwise Clustering (PC), while the second approach utilized a Time Series Clustering (TSC) method, which possesses the capability of incorporating temporal information. To prevent a major influence of the algorithms itself, it was essential to assess the efficacy of the two approaches using the same base algorithm. Consequently, a comparison was made between the well-known K-means algorithm (Lloyd, 1982) and a time series version of the same algorithm implemented by Király et al. (2024). To ensure that the algorithms were well-fitted, both were run 1000 times with different centroid seeds for 100 iterations each. The number of clusters (K) was set to the number of tested genotypes because the primary objective of this study was to analyze the impact of temporal data on genotype differentiation. This is in contrast to the investigation of present growth type groups, as performed by Chen et al. (2024). Euclidean distance was utilized as the scoring criterion for both approaches. Time series-specific metrics, such as Dynamic Time Warping, were considered unsuitable for this dataset due to the experimental design, which ensured temporal alignment of plant development by simultaneous sowing.

The data base for PC consisted of a single point in time, whereas TSC was provided with accumulated data extending from the initial data collection (37 DAS) to the respective time point analyzed. Additionally, the time series dataset was smoothed using a moving average filter with a window size three to remove noise and

reveal the underlying structure of the time series. Both clustering approaches were executed three times with different genotype groups, which means that initially, all twelve cultivated genotypes were clustered, and subsequently the two groups of breeding and market genotypes were clustered separately.

To investigate the impact of reduced data sampling intervals and determine the necessary temporal information for efficient 4D plant phenotyping, the TSC was repeated using only every second recorded time point. This resulted in one data collection per week. All other parameters of the algorithm were kept constant.

Feature Selection

Besides providing valuable insights into parameter importance development, the feature importance was additionally used in the feature selection process for both described clustering approaches. This was motivated by evidence that redundant features have the potential to influence unsupervised clustering algorithms, thereby resulting in a reduction in clustering performance (Hancer et al., 2020). The selection process encompasses two steps.

In the first step, a correlation analysis was performed individually for all time points to remove redundant information and reduce the dimensionality of the dataset. For each pair of parameters that correlated with a Pearson correlation coefficient of 0.95, the mean correlation of the two parameters with all other parameters was calculated. Consequently, the parameter with the higher mean correlation was removed from the dataset. The chosen threshold ensured an extensive reduction in the dimensionality of the dataset and that the remaining variables retained the greatest possible variance of the original dataset.

In the second step, the importance of the remaining parameters was calculated as described above to eliminate parameters that were considered insignificant for genotype differentiation. As a threshold for feature selection, the critical F-value derived from the previous analysis of variance was calculated on a significance level of $\alpha = 0.001$. The high significance level was selected to eliminate a considerable number of parameters. Nevertheless, the minimum number of parameters to use during clustering was set to nine according to findings of Hua et al. (2005). In this instance, the parameters were selected in descending order measured by their F-value. The implementation of the feature selection in the PC workflow was straightforward, as correlated and dispensable parameters could simply be excluded from further analysis. However, parameters could not be removed from the dataset for TSC, as their importance may fluctuate over time. Instead, values of parameters considered insignificant on a given time point were set to zero across all genotypes, removing their explanatory power only at specific time points, therefore allowing for dynamic parameter utilization in TSC.

To assess the efficacy of the proposed method for feature selection, both the PC and TSC clustering approaches were repeated and executed with and without feature selection. All other parameters of the algorithm were kept constant. Moreover, to compare the influence of the different observation scales of the plant and leaf parameters on genotype differentiation, both clustering approaches were repeated using either the one or the other parameter type. All other parameters of the algorithm were kept constant.

Performance Evaluation

The evaluation of both clustering approaches was conducted using the Adjusted Rand Index (ARI) (Hubert et al., 1985), as the genotype of each plant was known. The ARI measures the similarity between two clusterings by comparing pairs of samples and assessing the agreement between their cluster assignments on a scale between -1 and +1. As the ARI is label-independent, it is an effective metric for evaluating unsupervised clustering algorithms. Unlike the Rand Index, which suffers from scaling issues, the ARI adjusts for the similarity that could occur by chance (Steinley, 2004). It is calculated according to Hubert et al. (1985) as follows:

$$ARI = \frac{\sum_{ij}\binom{n_{ij}}{2} - \left[\sum_i \binom{a_i}{2} \sum_j \binom{b_j}{2}\right] / \binom{n}{2}}{\frac{1}{2}\left[\sum_i \binom{a_i}{2} + \sum_j \binom{b_j}{2}\right] - \left[\sum_i \binom{a_i}{2} \sum_j \binom{b_j}{2}\right] / \binom{n}{2}} \quad (3)$$

where:

- n_{ij} is the number of elements in the intersection between cluster i in the true labels and cluster j in the predicted labels
- a_i is the sum of elements in cluster i of the true labels
- b_j is the sum of elements in cluster j of the predicted labels
- n is the total number of data points
- $\binom{n}{2}$ is the binomial coefficient, which counts the number of ways to choose two elements from n

Trajectory Analysis

To analyze the development and the morphological relationships of the tested genotypes over time, unsupervised Uniform Manifold Approximation and Projection (UMAP) (McInnes et al., 2018) was applied to reduce the dimensionality of the collected dataset down to two dimensions. This enabled a visual inspection of the genotype trajectories, giving information about morphological relatedness and processes taking place. In contrast to a Principal Component Analysis, UMAP offers the advantage of preserving both local and global

relationships. Furthermore, it provides enhanced adaptability to a dataset through its customizable hyperparameters, leading to more interpretable and visually distinct illustrations. UMAP performs a nonlinear dimensional reduction, making it particularly well-suited for datasets with complex nonlinear relationships, such as growth patterns in plant phenotyping. To generate genotype-specific trajectories, the repetitions of each genotype were averaged for each time point. Subsequently, the UMAP embedding was calculated in an unsupervised manner, employing the following hyperparameters*:* *n_components*=2, *n_neighbors*=10, *min_dist*=0.99. As UMAP was used exclusively for visualization purposes, the hyperparameters were manually tuned to adequately depict the relationships of the genotypes and how they interrelate, while preventing a clumpy embedding and focusing on the broad topological structure to carve out the genotypic trajectories.

Results

Parameter Validation

The tests for extraction stability of the morphological parameters show, that most parameters exhibit a low CV of less than 5 %, with some parameters displaying a higher CV between 5 and 10 %, and a few even exceeding this range (Table 3). In general, it can be demonstrated that the CV increases with the complexity of the parameter calculation. Additionally, the CV is high for parameters including the calculation of the interquartile range (IQR) or the standard deviation (SD).

The results of the MRE calculation demonstrate a dispersed pattern, with numerous values surpassing the 10 % mark, indicating a discrepancy between the benchmark values and the recorded parameters. The highest MRE is observed for NORMAL ANGLE KURTOSIS, with a value exceeding 81 %. In a similar manner to the CV, the MRE increases with the complexity of parameter calculation. Furthermore, leaf-based parameters exhibited higher MRE values compared to plant-based parameters. In accordance with these findings, 7 out of 58 parameters were excluded from further analysis due to a CV greater than 10 % (see Table 3).

Parameter Importance

The results of the parameter importance analysis demonstrate noticeable differences in the importance of leaf parameters compared to plant parameters (see Figure S1 - Figure S3). Figure 5 depicts the dominant trends in parameter importance development. The leaf parameters show an overall lower importance and a higher short range temporal variability. Only one leaf parameter exceeds the feature selection threshold at all recorded time points. In general, a trend of decreasing leaf parameter importance over time is visible.

Table 3: Coefficient of Variation (CV) and Mean Relative Error (MRE) of plant and leaf morphological parameters extracted from 15 3D models of the 3D printed sugar beet reference model. Parameters excluded from further analysis are marked with a (†). (IQR: Interquartile Range, SD: Standard Deviation).

Parameter	CV[%]	MRE[%]	Parameter	CV[%]	MRE[%]
Height Maximum	0.58	2.01	Convex Hull Surface Volume	1.53	4.95
Height Mean	2.47	2.18	Convex Hull Surface Compactness	0.56	0.47
Height IQR	4.08	6.65	Convex Hull Surface Perimeter	0.25	1.16
Height SD	2.53	6.15	Leaf Quantity	0.00	0.00
Width Major Axis	0.30	1.14	Gap Fraction 3D	4.48	17.80
Width Minor Axis	5.26	8.03	Leaf Spacing	1.17	6.57
Width Aspect Ratio	5.37	9.01	Projected Leaf Area Mean	4.56	13.54
Height-Width Index	1.24	1.04	Leaf Overlap Area	1.01	7.66
Radius Maximum	0.73	2.27	Leaf Length Maximum	0.70	7.40
Radius Mean	2.67	8.87	Leaf Length Mean	0.54	10.31
Radius IQR	2.23	2.98	Leaf Length IQR	8.71	13.28
Radius SD	2.18	1.53	Leaf Length SD	2.12	7.04
Roundness	2.25	2.79	Blade Length Maximum	2.16	12.97
Height-Radius Index	1.57	2.08	Blade Length Mean	1.78	6.85
Height-Radius-Mean Index	3.57	9.13	Blade Length IQR (†)	13.39	31.28
Spatial Extent Maximum	0.79	1.02	Blade Length SD	3.89	21.58
Spatial Extent Mean	1.64	3.40	Stem Length Maximum	2.22	29.08
Spatial Extent IQR	3.78	19.82	Stem Length Mean	0.96	27.51
Spatial Extent SD	4.05	10.93	Stem Length IQR (†)	10.60	18.12
Points Quantity	6.56	18.00	Stem Length SD	2.62	2.98
Normal Angle Mean	2.15	7.72	Blade Width Maximum (†)	23.82	76.71
Normal Angle IQR	4.41	11.07	Blade Width Mean	6.02	44.75
Normal Angle SD	2.83	2.97	Blade Width IQR (†)	12.16	36.64
Normal Angle Distribution Skewness (†)	10.48	21.62	Blade Width SD (†)	26.76	39.92
Normal Angle Distribution Kurtosis (†)	12.47	81.85	Leaf Area Maximum	2.78	15.01
Projected Leaf Area	4.56	13.54	Leaf Area Mean	2.87	11.02
Ground Cover Area	0.53	2.30	Leaf Area IQR	7.51	11.70
Gap Fraction	4.14	11.52	Leaf Area SD	2.01	16.32
Convex Hull Surface Area	0.99	3.25	Leaf Area Sum	5.82	10.98

This decreasing trend is also visible for plant parameters, as illustrated by the SPATIAL EXTENT MAXIMUM (Figure 5). A more evident example of this phenomenon is provided by the LEAF AREA SUM, which initially exhibits high importance for genotype differentiation in the early stages of the experiment but rapidly loses significance and falls below the selection threshold in the experiment's secondary phase.

Contrasting with the general trend of decreasing parameter importance over time, certain parameters demonstrate an initial rise in importance until approximately 58 DAS, subsequently joining the descending trend. An illustration of this is provided by the HEIGHT-RADIUS-MEAN INDEX (Figure 5). Conversely, the importance of LEAF QUANTITY, BLADE LENGTH IQR and BLADE LENGTH SD are the only plant parameters whose importance increases over time, with an abrupt rise in importance starting at 75 DAS.

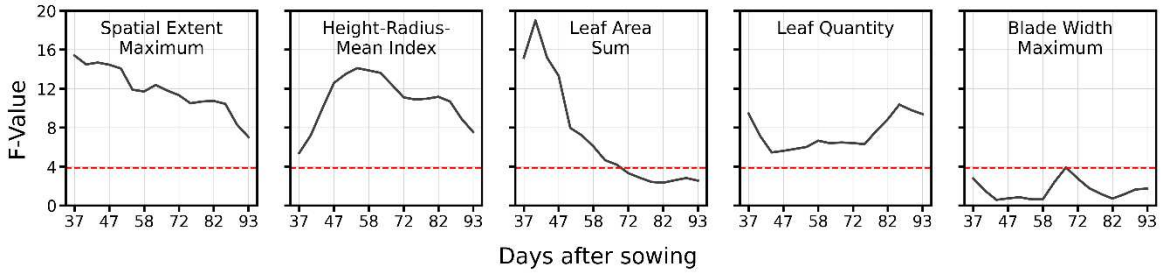

Figure 5: Importance of selected plant and leaf parameters measured over time. The red dotted line represents the critical F-value used as the feature selection threshold calculated at a significance level of $\alpha = 0.001$.

Clustering

Feature Selection

The tests for the effectiveness of the feature selection method proved, that the applied methods work as anticipated for most cases in both clustering approaches (see Table S1 and Table S2). The breeding genotypes benefit at all measured time points from feature selection using PC or TSC approaches. Furthermore, also the market genotypes reach higher performance scores at all time points when using TSC. All other clustering variants exhibited superior performance in at least two-thirds of the measured time points. Over all time points and variety combinations, PC gains about 11 % in clustering performance using feature selection, while TSC accomplishes 24 % better clustering results.

Performance Comparison of Clustering Algorithms

A comparison of PC and TSC clustering methods (see Figure 6) reveals that TSC provides a overall superior and temporally more stable clustering performance measured by the ARI, with reduced short- and long-term fluctuations. This phenomenon is particularly evident in the market genotype group. Additionally, a generally ascending trend in clustering performance is observed for all three genotype groups using TSC, while PC

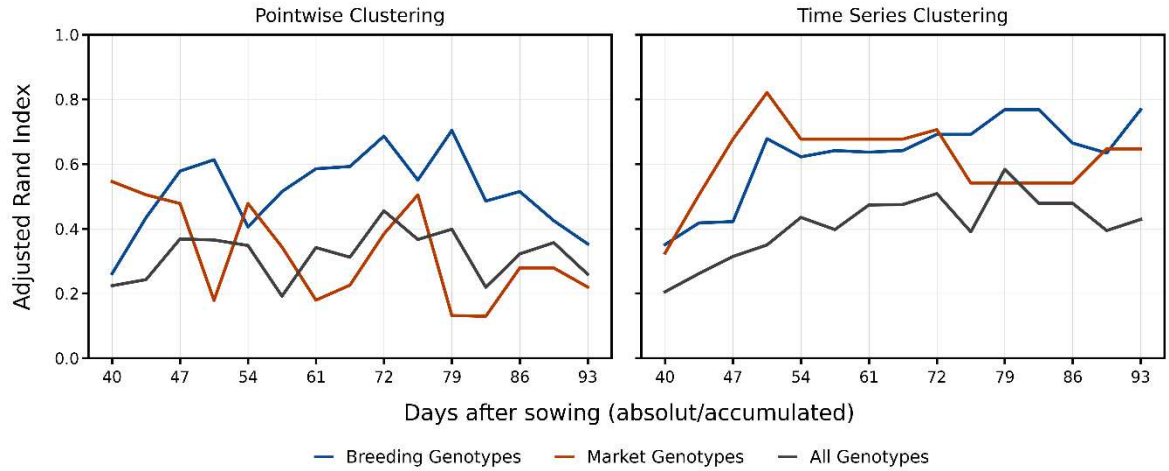

Figure 6: Adjusted Rand Index (ARI) over time for Pointwise Clustering (PC) (left side) and Time Series Clustering (TSC) (right side) using single plant and leaf parameters for breeding genotypes (blue), market genotypes (orange), and all genotypes combined (gray).

reveals no clear trend over the course of the experiment but rather experiences an unstable clustering with significant fluctuations of the ARI. Nevertheless, it can be observed that the performance of PC clustering for the market genotypes exhibits a decline over time.

The breeding genotypes exhibit a comparable increase in clustering performance for both methods until 51 DAS. However, this increase is lost over time for PC but is retained for the entire experiment for TSC. Similar to the breeding genotypes, the market genotypes show a notable performance gain measured by the ARI until 51 DAS. Subsequent to this, there is a slight decline in performance, yet it remains at a level that is comparable to the breeding genotypes. When all genotypes are considered collectively, the PC again fails to exhibit a distinct trend. However, TSC reveals a more stable clustering that exhibits a doubling in performance over the course of the experiment.

Clustering on Plant and Leaf Scale

For both clustering approaches, the employment of plant parameters almost consistently yields superior clustering performance (Table 4 and Table S3). The breeding genotypes can be separated with greater efficacy at any given time based on the plant parameters using PC and TSC, and the group encompassing all cultivated genotypes together follow this statement with the exception of one time point in the initial phase of the experiment.

However, for the market genotypes using TSC, a contrasting pattern is observed with better separation achieved by leaf parameters in the first half of the experiment. This pattern is also visible for the market

Table 4: Adjusted Rand Index (ARI) for Time Series Clustering (TSC). Comparison of using only plant or only leaf-based parameters across breeding, market, and all analyzed genotypes.

Days after sowing	Breeding		Market		All	
	Plant Parameter	Leaf Parameter	Plant Parameter	Leaf Parameter	Plant Parameter	Leaf Parameter
40	**0.22**	0.10	0.09	**0.44**	0.16	**0.19**
44	**0.31**	0.07	0.03	**0.44**	**0.24**	0.19
47	**0.47**	0.12	0.15	**0.39**	**0.44**	0.26
51	**0.68**	0.20	0.18	**0.48**	**0.38**	0.26
54	**0.62**	0.20	0.32	**0.48**	**0.43**	0.22
58	**0.62**	0.27	**0.31**	0.25	**0.33**	0.27
61	**0.64**	0.43	**0.40**	0.29	**0.47**	0.25
65	**0.64**	0.33	0.18	**0.18**	**0.42**	0.32
72	**0.68**	0.43	**0.38**	0.18	**0.40**	0.32
75	**0.67**	0.30	**0.54**	0.11	**0.59**	0.29
79	**0.80**	0.26	**0.54**	0.11	**0.59**	0.26
83	**0.72**	0.33	**0.54**	0.15	**0.51**	0.25
86	**0.72**	0.29	**0.54**	0.15	**0.55**	0.20
90	**0.64**	0.30	**0.65**	0.15	**0.44**	0.19
93	**0.62**	0.30	**0.65**	0.27	**0.44**	0.18

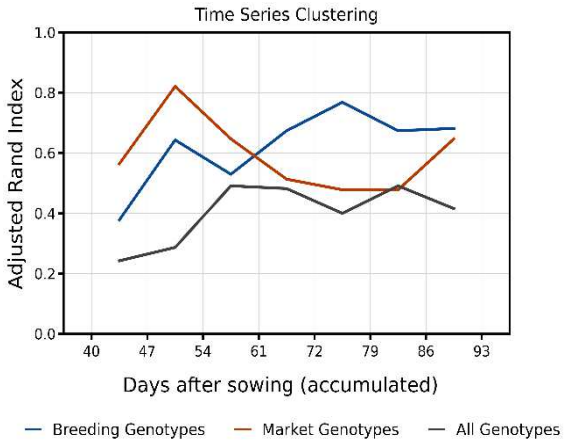

Figure 7: Adjusted Rand Index (ARI) over time for Time Series Clustering (TSC) using data from every second measurement date (seven-day interval) for breeding genotypes (blue), market genotypes (orange), and all genotypes combined (gray).

genotypes using PC at two time points at the beginning of the experiment. Nevertheless, clustering the market genotypes by plant parameters demonstrates significantly superior performance for the remaining duration of the experiment for both approaches.

Clustering on Reduced Time Series Data

An examination of the clustering performance with a reduced data basis shows a comparable systematic pattern for all three genotype combinations as when all available measurement time points were included (Figure 7). Both breeding and market genotypes reveals an initial period of rapid performance enhancement until 51 DAS. Subsequently, the breeding genotype demonstrates a sustained improvement in performance, while the market genotypes exhibit a slight decline. A comparison of the group clustering all genotypes reveals a stable performance that nearly doubles over the course of the experiment, as observed in the full-scale clustering.

Trajectory Analysis

The genotypic trajectories generated using UMAP reveal a generally aligned development in early stages of development, although the initial starting point differs for the breeding and market genotype groups (Figure 8). Subsequent to the first development, the breeding genotypes experience a fast spreading of their trajectories, resulting in an early split-off of genotypes one and four from the main group development at 44 and 47 DAS. Additionally, further separation of the morphological development of the breeding genotypes occurs around 54 DAS, as evident in the upper left part of the graphic where genotypes two, three, seven, and eight are diverging from each other. Furthermore, genotypes five and six undergo a rapid shift towards market genotypes during their development. The market genotypes exhibit a more uniform trajectory in the initial half of their development. However, analogous to the breeding genotypes, the market genotypes undergo a

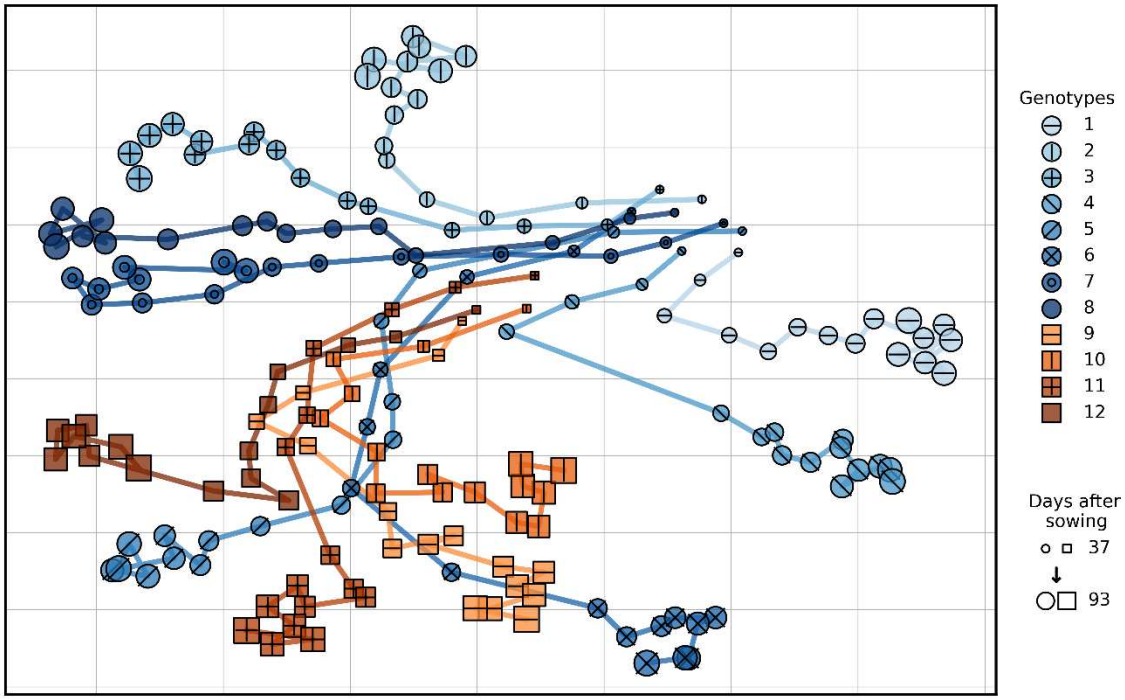

Figure 8: Two-dimensional UMAP visualization of genotype trajectories over time. Twelve different genotypes are visualized, blue colors indicate breeding genotypes, and orange colors indicate market genotypes. Data points are connected to represent temporal genotype development, with small points/squares indicating early and larger points/squares indicating later measurement dates.

separation during their development, which occurs around 58 DAS. Towards the end of the time series, starting at 75 to 79 DAS, the dynamic development of all genotypes slows down and they reach a stable position in space.

Discussion

Parameter Validation

A 3D printed reference model was used to assess the stability of parameter extraction, since only stable parameters contain valid morphological information. Parameters based on IQR or SD proved more error-prone, likely due to occlusion and uneven sampling under different scanning scenarios. Their use therefore requires high-quality data, which is difficult to achieve outdoors and in high throughput. While Weiss et al. (2010) demonstrated the importance of 3D distribution parameters, the results of this study highlight the difficulties in reliably extracting them. Thus, their implementation in phenotyping workflows must be executed with great caution.

A closer look at the leaf-based parameters showed higher MRE values compared to plant parameters. However, given the relatively low CV of these measurements, it is likely that systematic errors from differently defined key points are affecting the extraction rather than unstable extraction algorithms themselves. Henke

et al. (2022) similarly observed that higher-dimensional parameters exhibit greater deviations, which can be confirmed by the results of this study. This emphasizes the relevance of simple-to-extract morphological parameters for genotype differentiation.

The integration of a 3D printed reference model enables verifying novel 3D parameters previously not referenceable by conventional methods (Bömer et al., 2024). In this study, the process was found to be of great importance for identifying unstable-to-extract parameters and offering a more profound understanding of the schematic relationships between unstable feature acquisition and parameter construction.

Parameter Importance

The analyzed parameter importances displayed in Figure 5 and Figure S1 - Figure S3 show an overall lower importance of leaf based morphological parameters compared to plant based parameters. In contrast, several studies demonstrated that plant leaves can hold valuable phenotypic information. Wen et al. (2024) and Apelt et al. (2015) emphasized their overall relevance in maize and *A. thaliana*, while Milford et al. (1980) highlighted differences in expansion rate, final size, and dimensions (Milford et al., 1985) among different sugar beet genotypes. Moreover, (Bojović et al., 2019) reported significant variation in leaf number and area of sugar beet. Fellows et al. (1974) further described distinct temporal growth characteristics of sugar beet leaves during their transition from sink to source organs. In our study, clustering based on plant parameters consistently outperformed leaf-based clustering (Table 4, Table S3). However, in early growth stages, leaf parameters allowed better separation of hard-to-separate market genotypes, especially when using TSC. This underscores the significance of a comprehensive parameterization of crops for specific problems, such as genotype differentiation.

Furthermore, the conducted experiment did not encompass the entire growing period of sugar beet. In accordance with the findings of Milford et al. (1980) and Bojović et al. (2019), it can be hypothesized that leaf parameters regain importance in the later stages of sugar beet development. This claim is supported by the findings of Fellows et al. (1974), who described distinct temporal growth characteristics during the sink–source transition. Thus, further research is necessary to determine the temporal importance of leaf parameters for genotype differentiation.

In contrast, plant parameters exhibit a higher and more persistent importance over time, thereby more effectively capturing genotype specific growth patterns and structures of sugar beet. Figure 9 illustrates the potential of a 4D morphological analysis to capture dynamic growth patterns and genotype-specific structural development over time. Such 3D and 4D information are valuable for plant phenotyping, breeding, and

precision agriculture in general (Harandi et al., 2023). However, not all mensurable parameters are always beneficial for classification tasks. Therefore, the implementation of a variable feature selection approach for TSC has been shown to enhance clustering performance by more than 20%, thereby confirming the efficacy of a dynamically weighted parameter selection.

For both morphological parameter groups, a general decline in importance was observed after 58 DAS. This abrupt decline suggests a strong link of parameter importance to physiological processes and indicating that early stages are more informative for differentiation. Declines were likely caused by both convergence of parameter expression between genotypes (Chen et al., 2024) and increasing within-genotype variance (Michalska-Klimczak et al., 2020; Ma et al., 2025).

Across parameter groups, height, radius, and spatial extent were among the most influential features. Distributional parameters also showed high impact, consistent with (Weiss et al., 2010). In early developmental stages multiple parameters encompassing the leaf area also showed high importance, suggesting important genotypic differences in leaf development that can be utilized for genotype differentiation. Parameters derived from leaf segmentation, such as LEAF QUANTITY and LEAF SPACING, proved consistently important for genotype differentiation.

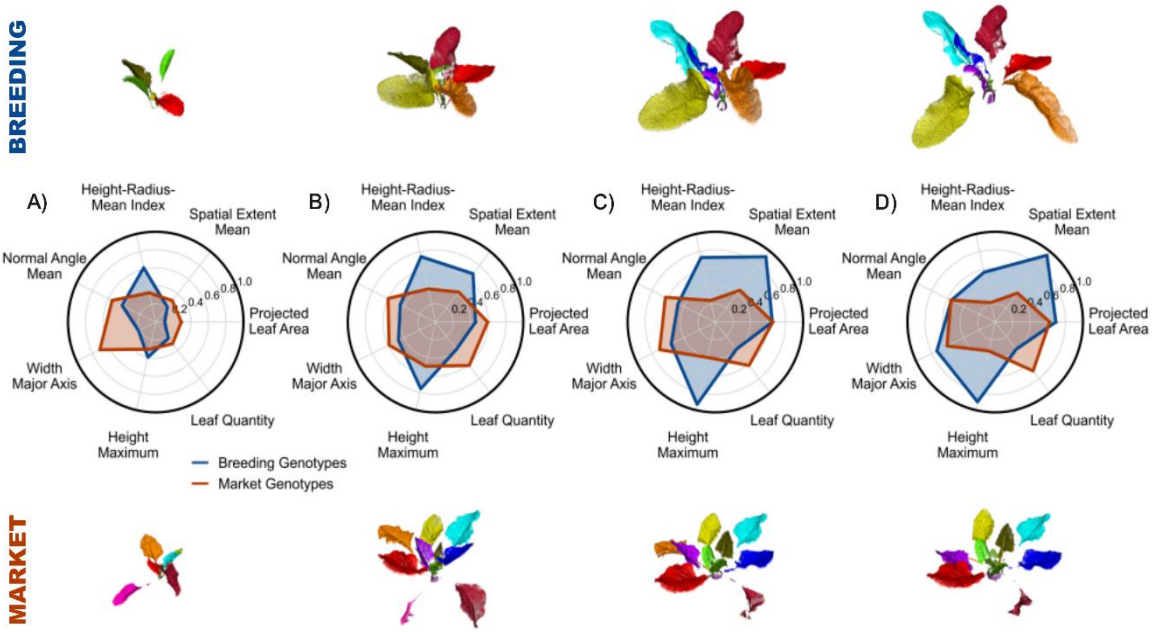

Figure 9: Subset of 3D morphological parameter expression for genotype four (breeding) and genotype ten (market) at four consecutive time points (40 days after sowing (DAS) (A), 54 DAS (B), 75 DAS (C) and 93 DAS (D)). Each panel includes a radar plot showing normalized morphological parameters and the corresponding annotated point clouds.

Evaluation of Clustering Approaches

The decreasing parameter importance affected both clustering approaches differently. PC demonstrated a slight decline in performance during the latter half of the experiment, while TSC performance exhibited an initial increase and subsequently stabilized (see Figure 6). This stable trend underscores the efficacy of incorporating temporal parameter development, as TSC integrates information across time rather than relying on a static measurement. Consequently, TSC was able to compensate for the reduced parameter importance and maintain high clustering performance.

The incorporation of time series data proves to be beneficial for all three tested genotype groups, particularly for the market genotypes that are difficult to separate. This finding underscores the advantage of spatio-temporal 4D phenotyping in the domain of plant breeding, as the temporal component provides additional information that facilitates the differentiation of morphologically closely related genotypes. The breeding genotypes primarily benefit from the stabilization of the clustering performance, as they are inherently separable due to their substantial morphological diversity.

The stabilization and enhancement of clustering performance underscores the relevance of time series analysis for practical applications in plant phenotyping and the evaluation of suggested candidates for variety approval. In this specific context, the findings reveal that the morphological parameters of sugar beets should not be assessed at a single point in time, but rather at multiple time points during the entire vegetation period. Our study demonstrates that even early growth stages are suitable for genotype differentiation. This finding aligns with the observations of Chen et al. (2024), who demonstrated that younger growth stages are more influenced by genotype and that the environmental influence on growth characteristics increases over time.

Genotypic Trajectories

In contrast to the market genotypes, the breeding genotypes exhibited a broader developmental pattern, which explains their superior initial performance in both clustering methods (Figure 8). Their trajectories revealed substantial morphological diversity, confirming the efficacy of the analysis and the existence of fundamental genotype-specific developmental patterns. By comparison, the market genotypes showed more uniform early development, reflecting the criteria underlying their initial selection for the experiment.

Beyond these general patterns, the trajectories also revealed the influence of a previously hypothesized physiological process shaping morphological parameter expression. A marked dispersal of trajectories was observed for both groups between 54 and 58 DAS, indicating a dominant physiological influence on leaf apparatus development. Previous studies suggest that this phase coincides with the onset of taproot formation.

Around 60 DAS, taproot growth accelerates exponentially (Hoffmann, 2006; Jammer et al., 2020; Kenter et al., 2006; Milford, 1973) and sugar accumulation increases rapidly (Jammer et al., 2020; Kenter et al., 2006). Hoffmann (2006) further showed that by 56 DAS cambium ring formation is well advanced and the number of leaves per ring is at its minimum, marking a shift in assimilate allocation from leaf growth to taproot development.

The divergent trajectories contrast with the simultaneous decrease in parameter importance. However, because Figure 8 reflects the full set of extracted parameters, separation among genotypes remains more robust than in importance estimates. This underlines the need for further research to clarify the dynamics of genotype-specific parameter expression and the precise role of taproot formation and other physiological processes.

Overall, the results demonstrate that taproot formation strongly affects leaf morphology. The declining momentum of trajectories towards the end of the experiment suggests that morphological development is largely complete and key differentiating traits are established. Nevertheless, it can be hypothesized that trajectories regain momentum later in the vegetation period, when leaf senescence and decreasing leaf area occur (Rinaldi, 2003; Tsialtas et al., 2007). These processes likely improve TSC performance, further strengthening genotype differentiation when the full growth period is considered.

Clustering with reduced data

To provide an initial assessment of the required temporal frequency of 3D data acquisition for genotype differentiation, the TSC workflow was repeated using only every second measurement date, resulting in one-week intervals. Despite the reduced information, the analysis still captured the same expressive parameter developments (Figure 7), indicating that high temporal frequency is not essential. This makes time series analysis highly suitable for practical breeding, as data collection efforts can be kept at manageable levels. Modern High-throughput Plant Phenotyping (HTPP) platforms already provide the necessary measurements and will become increasingly autonomous in the future (Atefi et al., 2021; Poorter et al., 2023; Watt et al., 2020). Moreover, they could be used to identify parameters that do require high frequency measurements. The findings indicate that these modern facilities will play a central role in collecting 4D datasets and providing developmental information for downstream plant phenotyping tasks.

Limitations and future research

The results of our study demonstrate a substantial impact of incorporating parameter development for genotype differentiation through a time series-based 4D analysis approach as compared to an approach focused on a discrete static time point. Nevertheless, there are specific aspects of our study that require further examination

to strengthen the underlying assumptions. These are based on only four experimental repetitions, making results sensitive to outliers and limiting representation of full morphological variability (Junker et al., 2015). Larger datasets with additional repetitions are required to improve general validity and enable advanced feature selection methods such as Recursive Feature Elimination (Guyon et al., 2002) or Boruta (Kursa et al., 2010).

Expanding the underlying database will also allow for the application of advanced supervised analytical algorithms, including Deep Learning, to investigate feature importance and temporal dynamics (Taghavi Namin et al., 2018). Opportunities for feature engineering across time, which transforms static into dynamic parameters, could additionally improve classification accuracy (Nanopoulos et al., 2001). While deep features may surpass handcrafted ones in predictive power, their integration into practical plant phenotyping requires careful consideration, since there are hard or even impossible to interpret.

Moreover, experiments were conducted under controlled greenhouse conditions, which restrict direct transferability to field environments (Heuermann et al., 2023). While greenhouse trials are valid and possess explanatory value, replicating the experiments in field environments, where they are subject to a variety of biotic and abiotic factors, would offer an increased practical relevance. However, the conventional outdoor cultivation techniques for sugar beet present a challenge to the extraction of the presented morphological parameters due to the restriction of the plants' undisturbed spatial development. Consequently, it is evident that not all of the morphological parameters presented can be transferred from the greenhouse to the field.

Future research should focus on optimizing the frequency of temporal data collection intervals. The results of this study have shown that a single data collection per week is sufficient for genotype differentiation. However, future studies must determine the optimal number of intervals or critical growth stages required for reliable 4D phenotyping, as Kierdorf et al. (2024) could show that limiting data collection to significant growth dates can enhance classification accuracy. Extending the method beyond plant and leaf scales to canopy and plot level, as shown for maize by Ma et al. (2024), offers additional potential. At the same time, finer leaf-level traits such as margin undulation or blistering (Community Plant Variety Office, 2018) remain promising but require high data quality for reliable extraction.

Conclusion

The present study demonstrates the superior performance and stability of genotype differentiation in sugar beet when spatio-temporal morphological growth data is integrated. TSC demonstrated clear superiority over

PC, particularly in the context of closely morphologically related genotypes, and its performance persisted even with reduced measurement frequency. These findings underscore the robustness of TSC and its practical applicability for phenotyping. Subsequent research should concentrate on the identification of key physiological growth stages to optimize data collection. In this study, taproot formation was identified as a pivotal event that significantly impacts genotype trajectories and leaf morphology.

A parameter importance analysis demonstrated that plant-level parameters had a greater impact on genotype differentiation than leaf-based parameters, supporting simplified data collection without the need for complex segmentation. The initial growth stages proved to be the most informative, as indicated by declining parameter importance over time and rapid clustering gains at the beginning of the experiment.

Overall, the study advances the understanding of morphological parameter development of sugar beet and underscores the importance of spatio-temporal 4D trait assessment for reliable plant phenotyping and variety approval. The results provide a foundation for further progress in plant breeding.

List of abbreviations

ARI	Adjusted Rand Index
CV	Coefficient of Variation
DAS	days after sowing
HTPP	High-throughput Plant Phenotyping
IQR	Interquartile Range
LiDAR	Light Detection and Ranging
MRE	Mean Relative Error
PC	Pointwise Clustering
SD	Standard Deviation
TSC	Time Series Clustering
UMAP	Uniform Manifold Approximation and Projection
2D	two-dimensional
3D	three-dimensional

4D	four-dimensional

Data availability

The generated point cloud dataset is available from the corresponding author on reasonable request and will be made publicly available in a follow-up publication. The extracted parameter values are included in the supplementary information files of this article, together with Python codes for reproducing the extraction of morphological plant parameters and the conducted analyses.

Supplementary materials

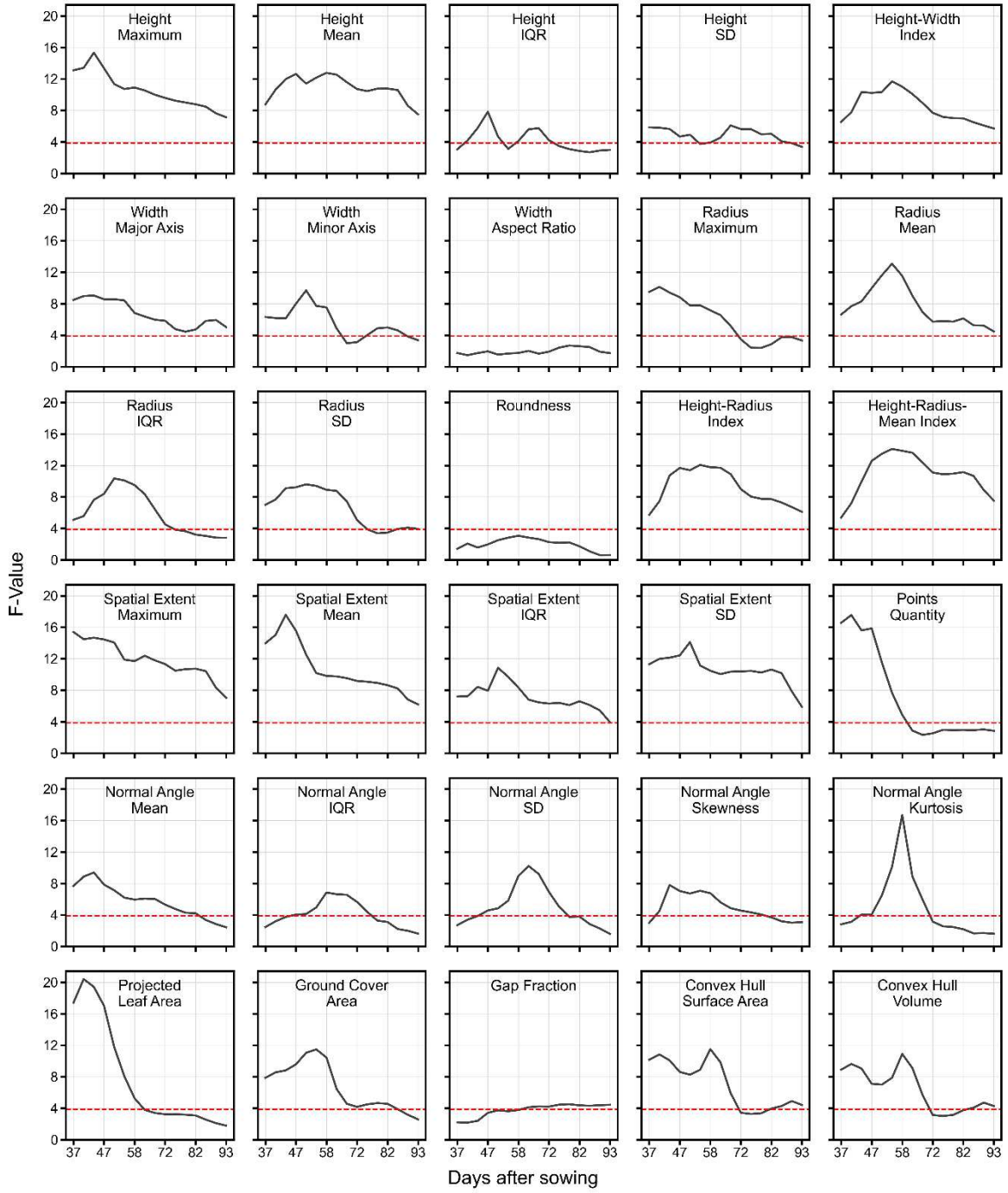

Figure S1: Importance of plant parameters (1-30) measured over time. The red dotted line represents the critical F-value used as the feature selection threshold calculated at a significance level of $\alpha = 0.001$ %. (IQR: Interquartile Range, SD: Standard Deviation).

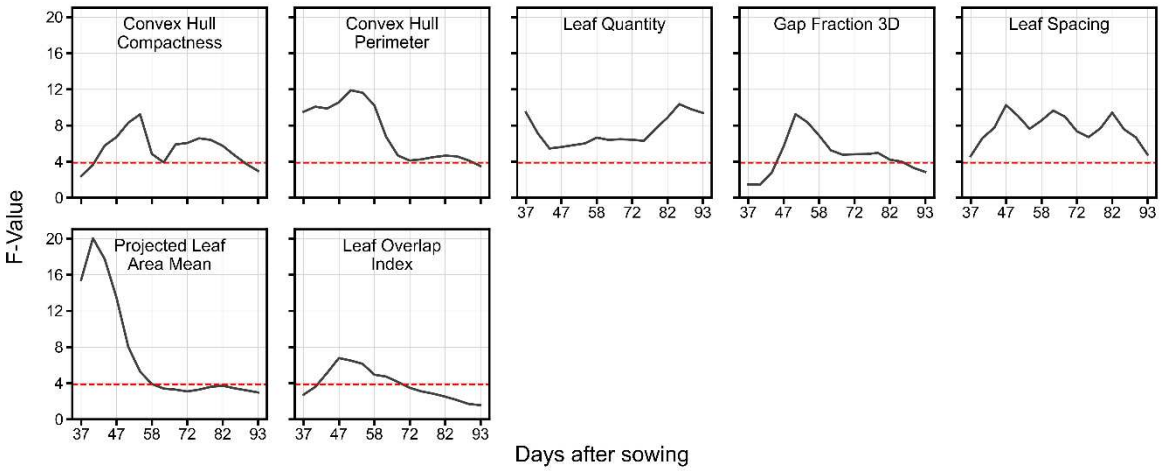

Figure S2: Importance of plant parameters (31-37) measured over time. The red dotted line represents the critical F-value used as the feature selection threshold calculated at a significance level of $\alpha = 0.001$ %.

1

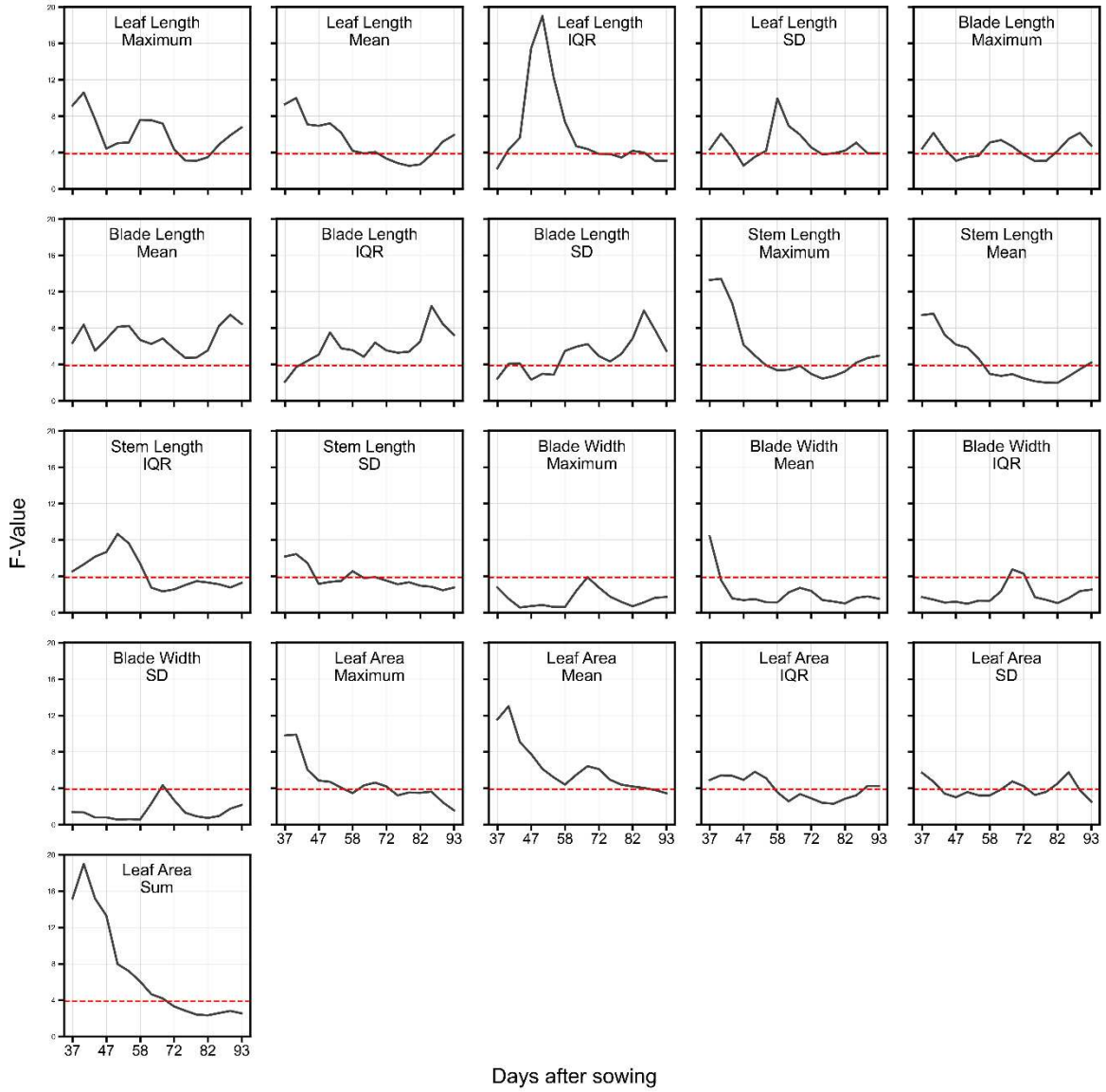

Figure S3: Importance of leaf parameters measured over time. The red dotted line represents the critical F-value calculated at a significance level of α = 0.001 %. (IQR: Interquartile Range, SD: Standard Deviation).

1

Table S1: Adjusted Rand Index (ARI) for Pointwise Clustering (PC). Comparison with and without feature selection across breeding, market, and all analyzed genotypes.

Days after sowing	Breeding		Market		All	
	Without Feature Selection	With Feature Selection	Without Feature Selection	With Feature Selection	Without Feature Selection	With Feature Selection
40	0.17	**0.26**	0.37	**0.55**	**0.32**	0.22
44	0.34	**0.43**	0.05	**0.50**	**0.30**	0.24
47	0.28	**0.58**	0.35	**0.48**	0.26	**0.37**
51	0.32	**0.61**	0.06	**0.18**	0.35	**0.37**
54	0.38	**0.41**	0.12	**0.48**	0.29	**0.35**
58	0.47	**0.51**	0.03	**0.34**	**0.28**	0.19
61	0.39	**0.58**	0.05	**0.18**	0.20	**0.34**
65	0.51	**0.59**	0.08	**0.23**	**0.33**	0.31
72	0.31	**0.69**	0.12	**0.38**	0.28	**0.46**
75	0.34	**0.55**	0.27	**0.50**	0.25	**0.37**
79	0.33	**0.70**	**0.25**	0.13	0.27	**0.40**
83	0.34	**0.49**	**0.48**	0.13	**0.25**	0.22
86	0.45	**0.51**	0.15	**0.28**	0.28	**0.32**
90	0.28	**0.42**	**0.28**	**0.28**	0.35	**0.36**
93	0.34	**0.35**	0.02	**0.22**	0.22	**0.26**

Table S2: Adjusted Rand Index (ARI) for Time Series Clustering (TSC). Comparison with and without feature selection across breeding, market, and all analyzed genotypes. Time series data is accumulated from time point 0 to *n*.

Days after sowing	Breeding		Market		All	
	Without Feature Selection	With Feature Selection	Without Feature Selection	With Feature Selection	Without Feature Selection	With Feature Selection
40	0.31	**0.35**	0.04	**0.32**	**0.29**	0.20
44	0.27	**0.42**	0.04	**0.50**	0.20	**0.26**
47	0.40	**0.42**	-0.01	**0.68**	**0.34**	0.31
51	0.32	**0.68**	0.04	**0.82**	**0.42**	0.35
54	0.24	**0.62**	0.06	**0.68**	0.34	**0.43**
58	0.32	**0.64**	0.11	**0.68**	0.27	**0.40**
61	0.47	**0.64**	0.11	**0.68**	0.37	**0.47**
65	0.45	**0.64**	0.11	**0.68**	0.46	**0.47**
72	0.56	**0.69**	0.11	**0.71**	0.38	**0.51**
75	0.49	**0.69**	0.23	**0.54**	**0.47**	0.39
79	0.54	**0.77**	0.23	**0.54**	0.47	**0.58**
83	0.51	**0.77**	0.32	**0.54**	0.40	**0.48**
86	0.57	**0.66**	0.20	**0.54**	0.38	**0.48**
90	0.57	**0.63**	0.34	**0.65**	0.37	**0.39**
93	0.57	**0.77**	0.08	**0.65**	0.38	**0.43**

Table S3: Adjusted Rand Index (ARI) for Pointwise Clustering (PC). Comparison of using only plant or only leaf-based parameters across breeding, market, and all analyzed genotypes.

Days after sowing	Breeding		Market		All	
	Plant Parameters	Leaf Parameters	Plant Parameters	Leaf Parameters	Plant Parameters	Leaf Parameters
40	**0.22**	0.04	**0.41**	0.31	**0.24**	0.10
44	**0.43**	0.05	0.12	**0.41**	**0.27**	0.15
47	**0.51**	0.27	**0.32**	0.12	**0.34**	0.21
51	**0.43**	0.23	0.18	**0.48**	**0.28**	0.23
54	**0.42**	0.32	**0.36**	0.08	**0.23**	0.22
58	**0.52**	0.20	**0.25**	0.00	**0.19**	0.13
61	**0.55**	0.14	**0.37**	0.04	**0.28**	0.17
65	**0.62**	0.14	**0.23**	0.20	**0.39**	0.17
72	**0.65**	0.22	**0.38**	0.20	**0.39**	0.09
75	**0.36**	0.10	**0.21**	0.03	**0.37**	0.00
79	**0.73**	0.13	**0.35**	0.11	**0.40**	0.06
83	**0.31**	0.18	**0.38**	0.08	**0.27**	0.18
86	**0.48**	0.20	**0.28**	0.13	**0.30**	0.16
90	**0.45**	0.22	**0.13**	0.10	**0.29**	0.09
93	**0.35**	0.16	**0.22**	-0.02	**0.21**	0.10

References

Akhtar, M. S., Zafar, Z., Nawaz, R., & Fraz, M. M. (2024). Unlocking plant secrets: A systematic review of 3D imaging in plant phenotyping techniques. *Computers and Electronics in Agriculture*, *222*, 109033. doi: https://doi.org/10.1016/j.compag.2024.109033

Apelt, F., Breuer, D., Nikoloski, Z., Stitt, M., & Kragler, F. (2015). Phytotyping4D: a light-field imaging system for non-invasive and accurate monitoring of spatio-temporal plant growth. *The Plant Journal*, *82*(4), 693–706. doi: https://doi.org/10.1111/tpj.12833

Atefi, A., Ge, Y., Pitla, S., & Schnable, J. (2021). Robotic technologies for high-throughput plant phenotyping: Contemporary reviews and future perspectives. *Frontiers in Plant Science*, *12*, 611940. doi: https://doi.org/10.3389/fpls.2021.611940

Awada, L., Phillips, P. W. B., & Smyth, S. J. (2018). The adoption of automated phenotyping by plant breeders. *Euphytica*, *214*, 1–15. doi: https://doi.org/10.1007/s10681-018-2226-z

Biskup, B., Scharr, H., Schurr, U., & Rascher, U. W. E. (2007). A stereo imaging system for measuring structural parameters of plant canopies. *Plant, Cell & Environment*, *30*(10), 1299–1308. doi: https://doi.org/10.1111/j.1365-3040.2007.01702.x

Bojović, R., Popović, V., Janković, S., Rajičić, V., Ikanović, J., Remiković, M. A., & Simić, D. (2019). Effect of genotype on morphological and quality features of sugar beet. *Agriculture & Forestry*, *65*(2), 29–38. doi: https://doi.org/10.17707/AgricultForest.65.2.02

Bömer, J., Esser, F., Marks, E., Rosu, R. A., Behnke, S., Klingbeil, L., Kuhlmann, H., Stachniss, C., Mahlein, A.-K., & Paulus, S. (2024). A 3D printed plant model for accurate and reliable 3D plant phenotyping. *GigaScience*, *13*, giae035. doi: 10.1093/gigascience/giae035

Breiman, L. (2001). Random forests. *Machine Learning*, *45*, 5–32. doi: https://doi.org/10.1023/A:1010933404324

Chen, H., Zhang, M., Xiao, S., Wang, Q., Cai, Z., Dong, Q., Feng, P., Shao, K., & Ma, Y. (2024). Quantitative analysis and planting optimization of multi-genotype sugar beet plant types based on 3D plant architecture. *Computers and Electronics in Agriculture*, *225*, 109231. doi: https://doi.org/10.1016/j.compag.2024.109231

Community Plant Variety Office. (2010). *Protocol for distinctness, uniformity and stability tests: Zea mays L .* Retrieved from https://cpvo.europa.eu/sites/default/files/documents/zea_mays_3_0.pdf

Community Plant Variety Office. (2018). *Protocol for tests on distinctness, uniformity and stability: Beta vulgaris L. ssp. vulgaris var. altissima Döll*. Retrieved from https://cpvo.europa.eu/sites/default/files/documents/beta_vulgaris_sugarbeet_1.2_0.pdf

Community Plant Variety Office. (2019). *Protocol for distinctness, uniformity and stability tests: Triticum aestivum L. emend. Fiori et Paol.* Retrieved from https://cpvo.europa.eu/sites/default/files/documents/triticum_aestivum_5.pdf

Community Plant Variety Office. (2025a). *Protocol for tests on distinctness, uniformity and stability: Brassica napus L. ssp. napus*. Retrieved from https://cpvo.europa.eu/sites/default/files/documents/2025-04/brassica-napus-4.pdf

Community Plant Variety Office. (2025b). *Protocol for tests on distinctness, uniformity and stability: Capsicum annuum L.* Retrieved from https://cpvo.europa.eu/sites/default/files/documents/2025-04/capsicum-annuum-3.pdf

Community Plant Variety Office. (2025c). *Protocol for tests on distinctness, uniformity and stability: Solanum lycopersicum L.* Retrieved from https://cpvo.europa.eu/sites/default/files/documents/2025-05/solanum-lycopersicum-5_1.pdf

Costa, C., Schurr, U., Loreto, F., Menesatti, P., & Carpentier, S. (2019). Plant Phenotyping Research Trends, a Science Mapping Approach. *Frontiers in Plant Science*, *9*. doi: https://doi.org/10.3389/fpls.2018.01933

Fellows, R. J., & Geiger, D. R. (1974). Structural and physiological changes in sugar beet leaves during sink to source conversion. *Plant Physiology*, *54*(6), 877–885. doi: https://doi.org/10.1104/pp.54.6.877

Fiorani, F., & Schurr, U. (2013). Future Scenarios for Plant Phenotyping. *Annual Review of Plant Biology*, *64*(Volume 64, 2013), 267–291. doi: https://doi.org/10.1146/annurev-arplant-050312-120137

Fischler, M. A., & Bolles, R. C. (1987). Random Sample Consensus: A Paradigm for Model Fitting with Applications to Image Analysis and Automated Cartography. In M. A. Fischler & O. Firschein (Eds.), Readings in Computer Vision (pp. 726–740). San Francisco (CA): Morgan Kaufmann. doi: https://doi.org/10.1145/358669.358692

Guyon, I., Weston, J., Barnhill, S., & Vapnik, V. (2002). Gene Selection for Cancer Classification using Support Vector Machines. *MMachine Language*, *46*(1–3), 389–422. doi: https://doi.org/10.1023/A:1012487302797

Hancer, E., Xue, B., & Zhang, M. (2020). A survey on feature selection approaches for clustering. *Artificial Intelligence Review*, *53*(6), 4519–4545. doi: https://doi.org/10.1007/s10462-019-09800-w

Harandi, N., Vandenberghe, B., Vankerschaver, J., Depuydt, S., & Van Messem, A. (2023). How to make sense of 3D representations for plant phenotyping: a compendium of processing and analysis techniques. *Plant Methods*, *19*(1), 60. doi: https://doi.org/10.1186/s13007-023-01031-z

Harris, C. R., Millman, K. J., der Walt, S. J. van, Gommers, R., Virtanen, P., David Cournapeau, Wieser, E., Taylor, J., Sebastian Berg, Smith, N. J., Kern, R., Hoyer, M. P. and S., van Kerkwijk, M. H., Matthew Brett, Haldane, A., del Río, J. F., Wiebe, M., Peterson, P., Pierre Gérard-Marchant, … Oliphant, T. E. (2020). Array programming with NumPy. *Nature*, *585*(7825), 357–362. doi: https://doi.org/10.1038/s41586-020-2649-2

Henke, M., & Gladilin, E. (2022). Virtual Laser Scanning Approach to Assessing Impact of Geometric Inaccuracy on 3D Plant Traits. *Remote Sensing*, *14*(19), 4727. doi: https://doi.org/10.3390/rs14194727

Heuermann, M. C., Knoch, D., Junker, A., & Altmann, T. (2023). Natural plant growth and development achieved in the IPK PhenoSphere by dynamic environment simulation. *Nature Communications*, *14*(1), 5783. doi: https://doi.org/10.1038/s41467-023-41332-4

Hoffmann, C. (2006). *Zuckerrüben als Rohstoff: Die technische Qualität als Voraussetzung für eine effiziente Verarbeitung*. Göttingen (Germany): Weender Druckerei.

Hua, J., Xiong, Z., Lowey, J., Suh, E., & Dougherty, E. R. (2005). Optimal number of features as a function of sample size for various classification rules. *Bioinformatics*, *21*(8), 1509–1515. doi: https://doi.org/10.1093/bioinformatics/bti171

Hubert, L., & Arabie, P. (1985). Comparing partitions. *Journal of Classification*, *2*, 193–218. doi: https://doi.org/10.1007/BF01908075

Hunter, J. D. (2007). Matplotlib: A 2D graphics environment. *Computing in Science & Engineering*, *9*(3), 90–95. doi: https://doi.org/10.1109/MCSE.2007.55

Ispizua Yamati, F. R., Günder, M., Barreto, A., Bömer, J., Laufer, D., Bauckhage, C., & Mahlein, A.-K. (2024). Automatic scoring of Rhizoctonia crown and root rot affected sugar beet fields from orthorectified UAV images using Machine Learning. *Plant Disease*, *108*(3), 711–724. doi: https://doi.org/10.1094/PDIS-04-23-0779-RE

James, K. M. F., Heiwolt, K., Sargent, D. J., & Cielniak, G. (2025). Lincoln's Annotated Spatio-Temporal Strawberry Dataset (LAST-Straw). *Computer Vision – ECCV 2024 Workshops. ECCV 2024. Lecture Notes in Computer Science*, *15625*, 46–63. doi: https://doi.org/10.1007/978-3-031-91835-3_4

Jammer, A., Albacete, A., Schulz, B., Koch, W., Weltmeier, F., van der Graaff, E., Pfeifhofer, H. W., & Roitsch, T. G. (2020). Early-stage sugar beet taproot development is characterized by three distinct physiological phases. *Plant Direct*, *4*(7), e00221. doi: https://doi.org/10.1002/pld3.221

Junker, A., Muraya, M. M., Weigelt-Fischer, K., Arana-Ceballos, F., Klukas, C., Melchinger, A. E., Meyer, R. C., Riewe, D., & Altmann, T. (2015). Optimizing experimental procedures for quantitative evaluation of crop plant performance in high throughput phenotyping systems. *Frontiers in Plant Science*, *5*, 770. doi: https://doi.org/10.3389/fpls.2014.00770

Kenter, C., & Hoffmann, C. M. (2006). Seasonal patterns of sucrose concentration in relation to other quality parameters of sugar beet (Beta vulgaris L.). *Journal of the Science of Food and Agriculture*, *86*(1), 62–70. doi: https://doi.org/10.1002/jsfa.2332

Kierdorf, J., Junker-Frohn, L. V., Delaney, M., Olave, M. D., Burkart, A., Jaenicke, H., Muller, O., Rascher, U., & Roscher, R. (2023). GrowliFlower: An image time-series dataset for GROWth analysis of cauLIFLOWER. *Journal of Field Robotics*, *40*(2), 173–192. doi: https://doi.org/10.1002/rob.22122

Kierdorf, J., Stomberg, T. T., Drees, L., Rascher, U., & Roscher, R. (2024). Investigating the contribution of image time series observations to cauliflower harvest-readiness prediction. *Frontiers in Artificial Intelligence*, *7*. doi: 10.3389/frai.2024.1416323

Kim, J. Y. (2020). Roadmap to high throughput phenotyping for plant breeding. *Journal of Biosystems Engineering*, *45*, 43–55. doi: https://doi.org/10.1007/s42853-020-00043-0

Király, F., Löning, M., Bagnall, T., Middlehurst, M., Ganesh, S., Walter, M., Oastler, G., Ray, A., Lines, J., ViktorKaz, Mentel, L., Heidrich, B., Mishra, S., chrisholder, Bartling, D., Tsaprounis, L., RNKuhns, Gilbert, C., Baichoo, M., … Schäfer, P. (2024). *sktime/sktime: v0.30.1*. Zenodo. doi: https://doi.org/10.5281/zenodo.11479106

Kursa, M. B., Jankowski, A., & Rudnicki, W. R. (2010). Boruta - A System for Feature Selection. *Fundamenta Informaticae*, *101*(4), 271–285. doi: https://doi.org/10.3233/FI-2010-288

Lande, R. (1977). On comparing coefficients of variation. *Systematic Zoology*, *26*(2), 214–217. doi: https://doi.org/10.2307/2412845

Li, L., Zhang, Q., & Huang, D. (2014). A Review of Imaging Techniques for Plant Phenotyping. *Sensors*, *14*(11), 20078–20111. doi: https://doi.org/10.3390/s141120078

Lloyd, S. (1982). Least squares quantization in PCM. *IEEE Transactions on Information Theory*, *28*(2), 129–137. doi: https://doi.org/10.1109/TIT.1982.1056489

Lu, Y., & Young, S. (2020). A survey of public datasets for computer vision tasks in precision agriculture. *Computers and Electronics in Agriculture*, *178*, 105760. doi: https://doi.org/10.1016/j.compag.2020.105760

Lundberg, S. M., & Lee, S.-I. (2017). A unified approach to interpreting model predictions. In Proceedings of the 31st International Conference on Neural Information Processing Systems (Vol. 30). Red Hook, NY, USA: Curran Associates Inc. Retrieved from https://proceedings.neurips.cc/paper_files/paper/2017/file/8a20a8621978632d76c43dfd28b67767-Paper.pdf

Ma, H., Wen, W., Gou, W., Liang, Y., Zhang, M., Fan, J., Gu, S., Zhang, D., & Guo, X. (2024). Three-Dimensional Time-Series Monitoring of Maize Canopy Structure Using Rail-Driven Plant Phenotyping Platform in Field. *Agriculture*, *15*(1), 6. doi: https://doi.org/10.3390/agriculture15010006

Ma, H., Wen, W., Gou, W., Lu, X., Fan, J., Zhang, M., Liang, Y., Gu, S., & Guo, X. (2025). 3D time-series phenotyping of lettuce in greenhouses. *Biosystems Engineering*, *250*, 250–269. doi: https://doi.org/10.1016/j.biosystemseng.2025.01.004

Manthey, R., Kenter, C., Laufer, D., & Ladewig, E. (2021). Das integrierte Sortenprüfsystem Zuckerrübe–Wachsen mit den Herausforderungen. *Sugar Industry International*, *146*(11), 643–646. doi: https://doi.org/10.36961/si28061

Marks, E., Bömer, J., Magistri, F., Sah, A., Behley, J., & Stachniss, C. (2024). BonnBeetClouds3D: A Dataset Towards Point Cloud-based Organ-level Phenotyping of Sugar Beet Plants under Field Conditions. *2024 IEEE/RSJ International Conference on Intelligent Robots and Systems (IROS)*, 1804–1811. doi: https://doi.org/10.1109/IROS58592.2024.10802820

Marks, E., Magistri, F., & Stachniss, C. (2022). Precise 3D reconstruction of plants from UAV imagery combining bundle adjustment and template matching. *2022 International Conference on Robotics and Automation (ICRA)*, 2259–2265. doi: https://doi.org/10.1109/ICRA46639.2022.9811358

McInnes, L., Healy, J., Saul, N., & Großberger, L. (2018). UMAP: Uniform Manifold Approximation and Projection. *Journal of Open Source Software*, *3*(29), 861. doi: https://doi.org/10.21105/joss.00861

Michalska-Klimczak, B., Wyszyński, Z., Pačuta, V., Rašovsk\`y, M., & Brezovsk\`y, O. (2020). Within-field variability of plant and canopy traits of sugar beet and their relation to individual root mass during harvest. *Plant, Soil & Environment*, *66*(9). doi: https://doi.org/10.17221/325/2020-PSE

Milford, G. F. J. (1973). The growth and development of the storage root of sugar beet. *Annals of Applied Biology*, *75*(3), 427–438. doi: https://doi.org/10.1111/j.1744-7348.1973.tb07991.x

Milford, G. F. J., Pocock, T. O., RILEY, J., & Messem, A. B. (1985). An analysis of leaf growth in sugar beet. III. Leaf expansion in field crops. *Annals of Applied Biology*, *106*(1), 187–203. doi: https://doi.org/10.1111/j.1744-7348.1985.tb03108.x

Milford, G. F. J., & RILEY, J. (1980). The effects of temperature on leaf growth of sugar beet varieties. *Annals of Applied Biology*, *94*(3), 431–443. doi: https://doi.org/10.1111/j.1744-7348.1980.tb03959.x

Nanopoulos, A., Alcock, R., & Manolopoulos, Y. (2001). Feature-based classification of time-series data. In Information processing and technology (Vol. 10, Issue 3, pp. 49–61). Nova Science Publishers, Inc.

Paproki, A., Sirault, X., Berry, S., Furbank, R., & Fripp, J. (2012). A novel mesh processing based technique for 3D plant analysis. *BMC Plant Biology*, *12*, 1–13. doi: https://doi.org/10.1186/1471-2229-12-63

Paulus, S. (2019). Measuring crops in 3D: using geometry for plant phenotyping. *Plant Methods*, *15*(1), 103. doi: https://doi.org/10.1186/s13007-019-0490-0

Pedregosa, F., Varoquaux, G., Gramfort, A., Michel V. and Thirion, B., Grisel, O., Blondel, M., Prettenhofer P. and Weiss, R., Dubourg, V., Vanderplas, J., Passos, A., Cournapeau, D., Brucher, M., Perrot, M., & Duchesnay, E. (2011). Scikit-learn: Machine Learning in Python. *Journal of Machine Learning Research*, *12*, 2825–2830.

Pélabon, C., Hilde, C. H., Einum, S., & Gamelon, M. (2020). On the use of the coefficient of variation to quantify and compare trait variation. *Evolution Letters*, *4*(3), 180–188. doi: https://doi.org/10.1002/evl3.171

Pieruschka, R., & Schurr, U. (2019). Plant Phenotyping: Past, Present, and Future. *Plant Phenomics*, *2019*, 7507131. doi: https://doi.org/10.34133/2019/7507131

Poorter, H., Hummel, G. M., Nagel, K. A., Fiorani, F., von Gillhaussen, P., Virnich, O., Schurr, U., Postma, J. A., van de Zedde, R., & Wiese-Klinkenberg, A. (2023). Pitfalls and potential of high-throughput plant phenotyping platforms. *Frontiers in Plant Science*, *14*, 1233794. doi: https://doi.org/10.3389/fpls.2023.1233794

Rinaldi, M. (2003). Variation of specific leaf area for sugar beet depending on sowing date and irrigation. *Italian Journal of Agronomy*, *7*(1), 23–32.

Rusu, R. B., Marton, Z. C., Blodow, N., Dolha, M., & Beetz, M. (2008). Towards 3D Point cloud based object maps for household environments. *Robotics and Autonomous Systems*, *56*(11), 927–941. doi: https://doi.org/10.1016/j.robot.2008.08.005

Schunck, D., Magistri, F., Rosu, R. A., Cornelißen, A., Chebrolu, N., Paulus, S., Léon, J., Behnke, S., Stachniss, C., Kuhlmann, H., & others. (2021). Pheno4D: A spatio-temporal dataset of maize and tomato plant point clouds for phenotyping and advanced plant analysis. *Plos One*, *16*(8), e0256340. doi: https://doi.org/10.1371/journal.pone.0256340

Segments.ai. (2023). *Segments.ai data labeling platform*. Retrieved from https://segments.ai

Steinley, D. (2004). Properties of the hubert-arable adjusted rand index. *Psychological Methods*, *9*(3), 386. doi: https://doi.org/10.1037/1082-989X.9.3.386

Strothmann, W., Ruckelshausen, A., Hertzberg, J., Scholz, C., & Langsenkamp, F. (2017). Plant classification with in-field-labeling for crop/weed discrimination using spectral features and 3d surface features from a multi-wavelength laser line profile system. *Computers and Electronics in Agriculture*, *134*, 79–93. doi: https://doi.org/10.1016/j.compag.2017.01.003

Taghavi Namin, S., Esmaeilzadeh, M., Najafi, M., Brown, T. B., & Borevitz, J. O. (2018). Deep phenotyping: deep learning for temporal phenotype/genotype classification. *Plant Methods*, *14*, 1–14. doi: https://doi.org/10.1186/s13007-018-0333-4

Tardieu, F., Cabrera-Bosquet, L., Pridmore, T., & Bennett, M. (2017). Plant phenomics, from sensors to knowledge. *Current Biology*, *27*(15), R770–R783. doi: https://doi.org/10.1016/j.cub.2017.05.055

The pandas development team. (2024). *pandas-dev/pandas: Pandas*. Zenodo. doi: https://doi.org/10.5281/zenodo.10957263

Tsialtas, J. T., & Maslaris, N. (2007). Leaf shape and its relationship with Leaf Area Index in a sugar beet (Beta vulgaris L.) cultivar. *Photosynthetica*, *45*, 527–532. doi: https://doi.org/10.1007/s11099-007-0090-5

Van Rossum, G., & Drake, F. L. (2009). *Python 3 Reference Manual*. Scotts Valley, CA: CreateSpace. doi: https://dl.acm.org/doi/abs/10.5555/869369

Virtanen, P., Gommers, R., Oliphant, T. E., Haberland, M., Reddy, T., Cournapeau, D., Burovski, E., Peterson, P., Weckesser, W., Bright, J., van der Walt, S. J., Brett, M., Wilson, J., Millman, K. J., Mayorov, N., Nelson, A. R. J., Jones, E., Kern, R., Larson, E., … SciPy 1.0 Contributors. (2020). SciPy 1.0: fundamental algorithms for scientific computing in Python. *Nature Methods*, *17*, 261–272. doi: https://doi.org/10.1038/s41592-019-0686-2

Walter, A., Liebisch, F., & Hund, A. (2015). Plant phenotyping: from bean weighing to image analysis. *Plant Methods*, *11*, 14. doi: https://doi.org/10.3929/ethz-b-000099721

Watt, M., Fiorani, F., Usadel, B., Rascher, U., Muller, O., & Schurr, U. (2020). Phenotyping: New Windows into the Plant for Breeders. *Annual Review of Plant Biology*, *71*, 689–712. doi: https://doi.org/10.1146/annurev-arplant-042916-041124

Weiss, U., Biber, P., Laible, S., Bohlmann, K., & Zell, A. (2010). Plant species classification using a 3D LIDAR sensor and machine learning. *2010 Ninth International Conference on Machine Learning and Applications*, 339–345. doi: https://doi.org/10.1109/ICMLA.2010.57

Wen, W., Wang, J., Zhao, Y., Wang, C., Liu, K., Chen, B., Wang, Y., Duan, M., & Guo, X. (2024). 3D Morphological Feature Quantification and Analysis of Corn Leaves. *Plant Phenomics*, *6*, 225. doi: https://doi.org/10.34133/plantphenomics.0225

Young, T. J., Jubery, T. Z., Carley, C. N., Carroll, M., Sarkar, S., Singh, A. K., Singh, A., & Ganapathysubramanian, B. (2023). “Canopy fingerprints” for characterizing three-dimensional point cloud data of soybean canopies. *Frontiers in Plant Science*, *14*. doi: https://doi.org/10.3389/fpls.2023.1141153

Zhou, Q.-Y., Park, J., & Koltun, V. (2018). *Open3D: A Modern Library for 3D Data Processing*. doi: https://doi.org/10.48550/arXiv.1801.09847

Zhu, R., Sun, K., Yan, Z., Yan, X., Yu, J., Shi, J., Hu, Z., Jiang, H., Xin, D., Zhang, Z., Li, Y., Qi, Z., Liu, C., Wu, X., & Chen, Q. (2020). Analysing the phenotype development of soybean plants using low-cost 3D reconstruction. *Scientific Reports*, *10*, 7055. doi: https://doi.org/10.1038/s41598-020-63720-2